VERIFICATION OF NOVEL WNT/BETA-CATENIN PATHWAY TARGETS

by

Ayşe Nur Kayabaşı

B.S., Molecular Biology and Genetics, Istanbul Technical University, 2016

Submitted to the Institute for Graduate Studies in
Science and Engineering in partial fulfillment of
the requirements for the degree of
Master of Science

Graduate Program in Molecular Biology and Genetics

Boğaziçi University

2019

For those who can ride their bikes with no handlebars…

ACKNOWLEDGEMENTS

This project was supported by the funds of BAP project number 13123.

Ayşe Nur Kayabaşı was supported by a TUBITAK-BIDEP fellowship for his MSc. study.

ABSTRACT

VERIFICATION OF NOVEL WNT/BETA-CATENIN PATHWAY TARGETS

One of the most fundamental signal transduction cascades, the Wnt/β-catenin signaling pathway, is an evolutionary conserved pathway in vertebrates which controls embryonic development and adult homeostasis. Signaling through secreted glycoproteins of Wnt family results in translocation of the transcriptional activator β-catenin into the nucleus where it controls key developmental gene expression programs. Having an important role in tissue homeostasis, aberrant activation of Wnt/β-catenin signaling pathway is often linked to a wide variety of cancers. Mutations in target molecules of this pathway are identified to have tumorigenic effect.

Previous studies confirmed BRI3 (Brain Protein 3) and MGAT1 (Mannosyl (Alpha-1,3-)-Glycoprotein Beta-1,2-N-Acetylglucosaminyltransferase) genes to be novel transcriptional targets of Wnt/β-catenin pathway. Huh7 cells (hepatocellular cancer cell line) stably expressing either BRI3 or MGAT1 have greater proliferative and invasive capabilities compared to wildtype Huh7 cells, and when subcutaneously injected into NUDE/SCID mice resulted in larger tumor formation. In the light of these findings, tumors were subjected to RNA-Sequencing for further investigation. We observed differential expression of certain genes involved in several cellular pathways. Among these genes, we continued with YAP1, CSNK2B, and AFP in BRI3 expressing cells; and EDNRB, ADAM17, and HSPA8 in MGAT1 expressing cells. We validated differential expression levels by using Western Blot and qRT-PCR techniques. We further aim to shed light into the crosstalk between different signaling pathways involved in cancer progression.

ÖZET

YENİ WNT / BETA-CATENIN SİNYAL YOLAĞI HEDEFLERİNİN DOĞRULANMASI

En temel sinyal iletim basamaklarından biri olan Wnt/β-catenin, omurgalılarda embriyonik gelişimi ve yetişkin homeostazisini kontrol eden evrimsel olarak korunmuş bir sinyal yolağıdır. Doku homeostazında önemli bir role sahip olan Wnt/β-catenin sinyal yolağının anormal aktivasyonu birçok çeşit kanser ile bağlantılı olup, bu yolun hedef moleküllerindeki mutasyonların tümörijenik etkiye sahip olduğu belirlenmiştir.

Laboratuvarımızda yürütülen daha önceki çalışmalar BRI3 (Beyin Protein 3) ve MGAT1 (Mannosil (Alfa-1,3 -) - Glikoprotein Beta-1,2-N-Asetilglukosaminiltransferaz) genlerinin Wnt/β-katenin yolağının yeni transkripsiyonel hedefleri olduğunu doğruladı. BRI3 veya MGAT1'i stabil şekilde eksprese eden hepatosellüler kanser hücreleri Huh7'lerin, doğal fenotip Huh7 hücrelerine kıyasla daha proliferatif ve istilacı yeteneklere sahip olduğu ve deri altından NUDE/SCID farelere enjekte edildiğinde daha büyük tümör oluşumu ile sonuçlandığı görülmüştür. MGAT1 ve BRI3 genlerinin hepatoselüler kanser oluşumuna katkısını aydınlatabilmek için araştırmaları daha derine indirerek RNA-dizileme yöntemine başvurulmuştur. Çeşitli hücresel yolaklarda görev alan belirli genlerde, kontrol ve BRI3 veya MGAT1 genlerinden birinin aşırı anlatımının sağlandığı hücreler arasında diferansiyel ekspresyon seviyeleri gözlemlenmiştir. Western Blot ve qRT-PCR teknikleri kullanılarak bu diferansiyel ekspresyon seviyeleri doğrulanmıştır. Kanser oluşumunun altında yatan mekanizmayı ortaya çıkarabilmek adına protein-protein fiziksel etkileşimleri biyoinformatik olarak incelenmiş ve farklı kombinasyonlarda proteinlerarası etkileşim saptanmıştır. Literatür araştırması da dahil edilerek BRI3 ve MGAT1 genlerinin hepatosellüler kanser oluşumuna katkısı seçilen genler üzerinden incelenmiş, ve aydınlatılmaya çalışılmıştır.

TABLE OF CONTENTS

LIST OF FIGURES

LIST OF TABLES

LIST OF SYMBOLS

bp	Base pair
g	Gram
kb	Kilobase
kDa	Kilodalton
L	Liter
ml	Milliliter
mm	Millimeter
mM	Millimolar
min	Minutes
M	Molar
ng	Nanogram
nm	Nanometer
rpm	Revolutions per minute
v	Volume
w	Weight
µg	Microgram
µm	Micrometer
µl	Microliter

LIST OF ACRONYMS/ABBREVIATIONS

ADAM17	Adam metallopeptidase domain 17
AFP	Alpha fetoprotein
APGC	AFP-producing gastric cancer
ATRA	All-trans retinoic acid
BRI3	Brain protein 3
BAG1	Bcl2 associated athanogene 1
CSNK2β	Casein kinase 2β
CK2	Casein kinase holoenzyme
cDNA	Complementary DNA
ChIP	Chromosome immunoprecipitation
CMA	Chaperone-mediated autophagy
CNS	Central nervous system
DNA	Deoxyribonucleic acid
ET	Endothelin
EDNRB	Endothelin receptor type B
FC	Fold change
GFP	Green fluorescent protein
GO	Gene Ontology
GPCR	G-protein coupled receptor
HBV	Hepatitis B virus
HCV	Hepatitis C virus
HCC	Hepatocellular carcinoma
HSPA8	Heat-shock protein family A member 8
IKKε	Inhibitor of nuclear factor kappa-B kinase subunit epsilon
EMT	Epithelial to mesenchymal transition

LATS1/2	Large tumor suppressor kinase 1
LEF	Lymphoid enhancer binding factor
MGAT1	Mannosyl (alpha-1,3-)-glycoprotein beta-1,2-N-acetylglucosaminyl-transferase
MST1/2	Mammalian sterile 20-like 1/2
NAFDL	Nonalcoholic fatty liver disease
nt	Nucleotide
NFkB	Nuclear factor kappa B subunit 1
OLT	Orthotopic liver transplantation
PBS	Phosphate buffered saline
PLP	Planar polarity pathway
PCR	Polymerase chain reaction
pH	Power of hydrogen
qRT-PCR	Quantitative reverse transcription polymerase chain reaction
RNA	Ribonucleic acid
RNA-Seq	RNA Sequencing
RT	Room temperature
RT-PCR	Reverse transcription polymerase chain reaction
shRNA	Short hairpin ribonucleic acid
siRNA	Small interfering ribonucleic acid
TEAD	Transcriptional enhanced associate domain
TF	Transcription factor
TGF-β	Transforming growth factor-beta
VEGF	Vascular endothelial growth factor
YAP1	Yes-associated protein 1

1. INTRODUCTION

1.1. Cancer Overview

Cancer, also called malignancy, is a group of diseases associated with abnormal cell growth. In all types of cancer, some cells begin to divide uncontrollably and spread into other parts of the body. More than 100 specific types of cancer are found to affect humans and the symptoms may change due to the type of cancer. Cancer development is a multistep process including accumulation of mutations and selective increase in number of cells with increasing capacity for survival, proliferation, invasion capability, and metastatic properties (Cooper and Haussman, 2009).

Genes that are affected can be subcategorized as oncogenes and tumor suppressor genes. Oncogenes are the genes capable of inducing cell transformation through promoting cell growth and reproduction. As a result of genetic alterations which either lead to uncontrolled activity of oncogene-encoded proteins or increase gene expression, oncogenes drive abnormal cell proliferation. Tumor suppressor genes inhibit cell proliferation and survival under normal circumstances. Malignant transformation arises from overexpression of normal oncogenes, formation of novel oncogenes, inactivation of tumor suppressor genes, or under-expression of tumor suppressor genes (Knudson, 2001).

There are six hallmarks in cancer cells comprising unique and complementary capabilities acquired during the development of tumor that ensure the complexity of the disease. These include sustaining signaling that provide proliferation by deregulating the release of growth-promoting signals, evading growth suppressors by inactivating tumor suppressor genes, resisting programmed cell death, acquiring unlimited replicative potential, stimulation of angiogenesis, and activating local tissue invasion and formation of metastases (Hanahan and Weinberg, 2011)

1.2. Hepatocellular Carcinoma

The liver is made up of different kinds of cells. The type of cancer depends on which cells it starts in. There are hepatocellular carcinoma, fibrolamellar carcinoma, intra hepatic cholangiocarcinoma, angiosarcoma, and hepatoblastoma. Hepatoblastoma is formed by immature liver cells. Cancer of the bile duct is cholangiocarcinoma. The liver is 80-90% made up of hepatocytes, and the most frequent primary liver malignancy is hepatocellular carcinoma (HCC).

HCC is the fourth prominent cause of cancer deaths across the globe, accounting for 5% of all cancers. It is one of the deadliest cancers with 782,000 deaths in 2018 (World Health Organization, 2018). HCC occured more frequently in males than females, with a higher incidence rate in Middle and Western Africa, Eastern and Southern Asia, Micronesia/Polynesia, and Melanesia (Ferlay *et al.*, 2010). Even though prevention techniques in HCC, screening of the disease, and new technologies in treatment and diagnosis advanced, incidence of mortality persist to rise. A total of 42,220 new intrahepatic bile duct and liver cancers were expected to occur in 2018 in addition to 30,200 deaths (American Cancer Society, 2018). HCC carries a significant economic burden on society, most importantly in the East Asian countries where Hepatitis B infection (HBV) is endemic.

Cirrhosis is still counts as the most important risk and the main factor for the development of HCC, independent from etiology. Infections of Hepatitis B (HBV) and Hepatitis C (HCV) viruses, and chronic aflatoxin exposure lead to formation of cirrhosis; and make up 80% of all HCC cases. Nonalcoholic fatty liver disease (NAFDL), alcohol abuse, hereditary hemochromatosis, autoimmune hepatitis and Wilson's disease are also risk factors for the development of cirrhosis (Balogh *et al.*, 2016). Hepatocarcinogenesis almost always advances in the situations of cirrhosis or chronic hepatitis, caused by hepatocyte deaths in the

liver and invasion of inflammatory cells in the liver and the connective tissue surrounding it (Thorgeirsson and Grisham, 2002).

HBV is a virus that can integrate its double-stranded DNA into hepatocytes and acts as a mutagenic agent. In these cells, the virus causes secondary chromosomal rearrangements and results in genomic instability (Szabó *et al.*, 2004). As a result of both direct and indirect pathways, the risk of HCC development is 100-fold higher for HBV-infected patients compared

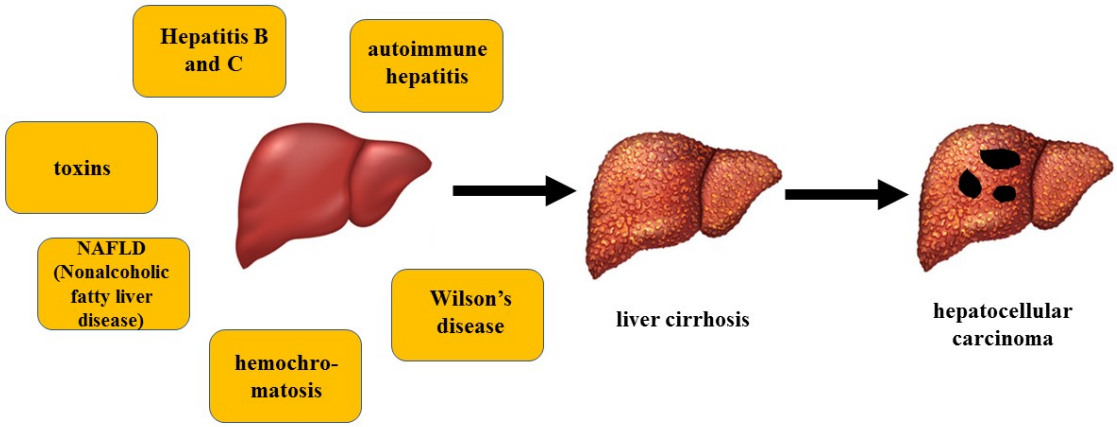

to uninfected (Herbst and Reddy, 2011). The risk becomes even higher for patients with an HBV infection and cirrhosis (Bruix and Sherman, 2005).

Figure 1.1. Risk factors for the development of liver cirrhosis with subsequent hepatocellular carcinoma (Uhl *et al.*, 2014).

The major cause of HCC in Europe, United States, Japan, and Latin America is HCV-associated cirrhosis with an estimated annual HCC incidence of 2% to 8% (Ferenci *et al.*, 2010). HCV is an RNA virus therefore unable to integrate itself into the host genome, but leads to HCC by several indirect mechanisms. For instance, it alters apoptotic pathways; HCV core protein localizes in the endoplasmic reticulum as well as in the outer mitochondrial membrane and stimulates oxidative stress, resulting in key signaling pathways activation and subsequently inflammation (Sheikh *et al.*, 2008). HCV-infected patients bear 17-fold higher risk of

developing HCC than those who are not infected (Herbst and Reddy, 2011) Researchers have also found correlation between obesity and diabetes mellitus with increased risk of HCC (Polesel *et al.*, 2009). Finally, smoking found to increase the risk of developing HCC in comparison with non-smokers (Chuang *et al*., 2009).

Hepatocarcinogenesis is rather a long process taking more than 30 years from the initiation to the malignant type. During this long preneoplastic stage, at when the liver is often the site of cirrhosis and/or chronic hepatitis, hepatocyte cycling is expedited by mitogenic pathways upregulation, mostly through epigenetic mechanisms. The genomic basis of the malignant type is heterogenous; however, development of dysplastic hepatocytes in nodules and hepatocarcinogenesis are associated with accumulated irreversible structural aberrations in genes as well as chromosomes (Cavin *et al.*, 2004).

HCC is asymptomatic in many patients and when symptoms can be observed, they are usually related to those of chronic liver disease such as pain in the right upper abdominal side, yellowing of the skin and eyes, swelling of the abdomen, weight loss, fever, weakness (El-Serag *et al*., 2008; Waly Raphael *et al.*, 2012).

An estimated 57% of the total hepatic cirrhosis and 78% of the hepatocellular carcinomas are the consequence of HBV and HCV infections (Perz *et al.*, 2006). This data shows the importance for hepatitis infections to be diagnosed at an early stage in order to provide optimal treatment to patients.

Because more than 80% of all HCC incidents begin with cirrhosis, and the risk of hepatocarcinogenesis increases to up to 5% each year in patients with cirrhotic liver, cirrhotic nodules may already contain genetic alterations and are apparently premalignant lesions before HCC (Hamilton, 2001).

Molecular mechanisms underlying HCC seems to involve complex network of different signaling pathways. Several signaling pathways including Wnt pathway, the Hedgehog

pathway, Hippo pathway and the TGF-β (transforming growth factor-beta) pathway are found to participate in the development of HCC (Caja *et al.*, 2007; Sun *et al*., 2015; Wang *et al*., 2013; Yimlamai *et al.*, 2015). Genetic and epigenetic alterations also lead to hepatocarcinogenesis through disruption of p53 and Rb1 pathways (Edamoto *et al*., 2003). Studies on mutational extends have mostly concentrated on several genes, TP53, CTNNB1, TERT, ARID1A, NFE2L2 and KEAP, listed in Table 1.

1.2.1. Treatment of Hepatocellular Carcinoma

Orthotopic liver transplantation (OLT) can be effective against both hepatocellular carcinoma and underlying cirrhosis for the early stages. But in most cases, cancers are in an advanced stage and metastasized when diagnosed, and are not suitable candidates for OLT (Forner, M Llovet, & Bruix, 2012).

Table 1.1 Most frequently mutated genes in hepatocellular carcinoma.

Pathways	Genes	Frequency in HCC (%)	References
	TERT	47.1	(Jhunjhunwala *et al.*, 2014)
Cell cycle control	TP53	28-36	(Boyault *et al.,* 2007)
	CCND1	7.2	(Llovet *et al.*, 2015)
	CDKN2A	7.2	(Guichard *et al*., 2012)
WNT-β-catenin signalling	CTTNB1	17-37	(Jhunjhunwala *et al.*, 2014; Schulze *et al.*, 2015)
	AXIN1	4-14	(Boyault *et al.*, 2007; Jhunjhunwala *et al*., 2014)
AKT-mTOR-MAPK pathway	RPS6KA3	2-10	(Boyault *et al.*, 2007; Guichard *et al.*, 2012)
	PTEN	3	(Schulze *et al.*, 2015)
	FGF19	5	(Schulze *et al.*, 2015)

Table 1.1 Genes most frequently mutated in hepatocellular carcinoma (cont.).

Chromatin remodeling	ARID1A	16.8	(Guichard *et al.*, 2012)
	ARID2	5.6	(Guichard *et al.*, 2012)
Oxidative stress	NFE2L2	6.4	(Guichard *et al.*, 2012)
	KEAP1	8	(Cleary *et al.*, 2013)
JAK/STAT signaling	JAK1	5	(Jhunjhunwala *et al.*, 2014)
Angiogenesis	VEGFA	3.8	(Chiang *et al.*, 2008)

Another treatment option for a small number of patients that has good liver function, single nodules and no underlying cirrhosis is surgical resection. Patients with cirrhosis have a higher risk of hepatic decompensation after surgical resection; hence only patients with well-compensated cirrhosis are considered the suitable candidates for this operation (Beard *et al.*, 2013; J. Bruix *et al.,* 1996). However, recurrence rate is much higher in the patients who undergo surgical resection in spite of 70% five-year survival (Barbier *et al.*, 2013).

Systemic targeted therapies for advanced HCC focus on the critical steps of carcinogenesis, reducing widespread systemic toxicity. The pathogenesis of HCC implements overexpression of multiple signaling pathways listed in Table 1. Targeted therapies provide anti-cancer management by blocking one or more steps in targeted pathways. Sorafenib is a receptor tyrosine kinase inhibitor having anti-angiogenic and pro-apoptotic activities; it shows improved overall survival and is the only drug approved by FDA so far, and many new therapies are currently being tested against HCC. Regorafenib, which is a multikinase inhibitor showed a broad spectrum of anti-tumor activity (including inhibition of angiogenesis and cell proliferation), as second-line treatment for advanced HCC (Wilhelm *et al.*, 2011).

1.3. Wnt Signaling Pathway

The Wnt pathway is a highly complex, evolutionary conserved signaling pathway activated by secreted Wnt ligands. There are 19 secreted cysteine-rich Wnt ligands, each having distinct, but overlapping functions, and >15 receptors varying in a broad spectrum and triggering different downstream signals (Logan & Nusse, 2004). The pathway is involved in many developmental processes as well as the maintenance of adult tissue homeostasis by regulating adult stem cells generation, cell proliferation, differentiation, migration, and apoptosis.

To this date, three different pathways are believed to be activated by Wnt ligands: the canonical Wnt pathway, the noncanonical planar polarity pathway (PCP), and the Wnt/Ca^{2+} pathway. Conventionally, the Wnt pathway is divided as the canonical (mediated through the transcriptional regulator β-catenin) and the noncanonical (independent of β-catenin) including both PCP and the Wnt/Ca^{2+} pathway (Kahn, 2014). β-catenin-independent Wnt pathways have vital roles in embryo morphogenesis through regulating directed cell migration, also in a context-dependent way, contribute to the migration and invasion of cancer cells. Alterations in these pathways such as differential expression of Wnt5a and Wnt11 can also result in thorough effects on cancer cell proliferation (Anastas & Moon, 2013).

1.4. The canonical Wnt/β-catenin signaling pathway

The key regulator of the canonical Wnt cascade is β-catenin whose cytoplasmic stability is controlled by the destruction complex. Axin is a tumor suppressor protein that acts as a scaffold in this complex as it physically interacts with all other components: β-catenin, tumor suppressor protein APC, and the two kinase families (CK1α, -δ, -ε and GSK3α and -β). Without Wnt ligand binding, β-catenin is sequentially phosphorylated by CK1 and GSK3α/β near its N-terminus. As a component of a E3 ubiquitin ligase complex, β-TrCP then recognizes the phosphorylated β-catenin. Consequently, β-catenin is ubiquitinated and targeted for proteasomal degradation (Aberle, Bauer, Kispert, & Kemler, 1997). Once bound by Wnt ligands, Frizzled/LRP co-receptor complex activates the canonical Wnt/β-catenin pathway and the signal

progresses through dissociation of the destruction complex. Wnt ligands induce the phosphorylation of LRP5/6 by GSK3β and CK1γ, which recruits Dvl to the plasma membrane. Dvl inactivates the destruction complex, regulating the recruitment of Axin to the plasma membrane, away from the destruction complex; in turn, leading to β-catenin stabilization and translocation into the nucleus. β-catenin acts as a transcriptional co-activator in the nucleus by binding to the TCF/LEF family of transcription factors and activates gene expression (Jürgen Behrens *et al*., 1996; Molenaar *et al.*, 1996; Yost *et al.*, 1996). The canonical Wnt signaling pathway regulates a variety of processes including cell proliferation, survival, and cell fate decisions (Kahn, 2014). A summary of the canonical Wnt/β-catenin signaling pathway is illustrated in Figure 1.2.

1.4.1. Major Components of the Canonical Wnt Pathway

Wnt ligands are cysteine-rich secreted proteins of 350-400 amino acids containing an N-terminal signal peptide. Wnts function as morphogens capable of short and long-range signaling. Two distinct cell surface receptors operate together to initiate Wnt signaling upon Wnt ligand binding. One of them is a member of the seven-pass Frizzled (Fz) family of serpentine proteins with a highly conserved amino-terminal cysteine rich domain, and the other is low-density lipoprotein (LDL) receptor-related protein 6 (LRP6) or closely related LRP5 that consists of a long single-pass transmembrane protein. Wnt stimulation induces a signal transduction through Fz-LRP6 complex formation, resulting in the recruitment and phosphorylation of the scaffold protein Dishevelled (Dsh). The activated receptor complex promotes the phosphorylation of LRP receptor by GSK3 and CK1. This phosphorylation recruits Axin to the receptor complex, thereby preventing the degradation of β-catenin in the cytoplasm (Alberts *et al.*, 2014). When bound to their respective membrane receptors, Axin and Dsh may collectively mediate downstream activation by forming a heterodimer through their respective Dishevelled-Axin (DIX) domains (Clevers, 2006).

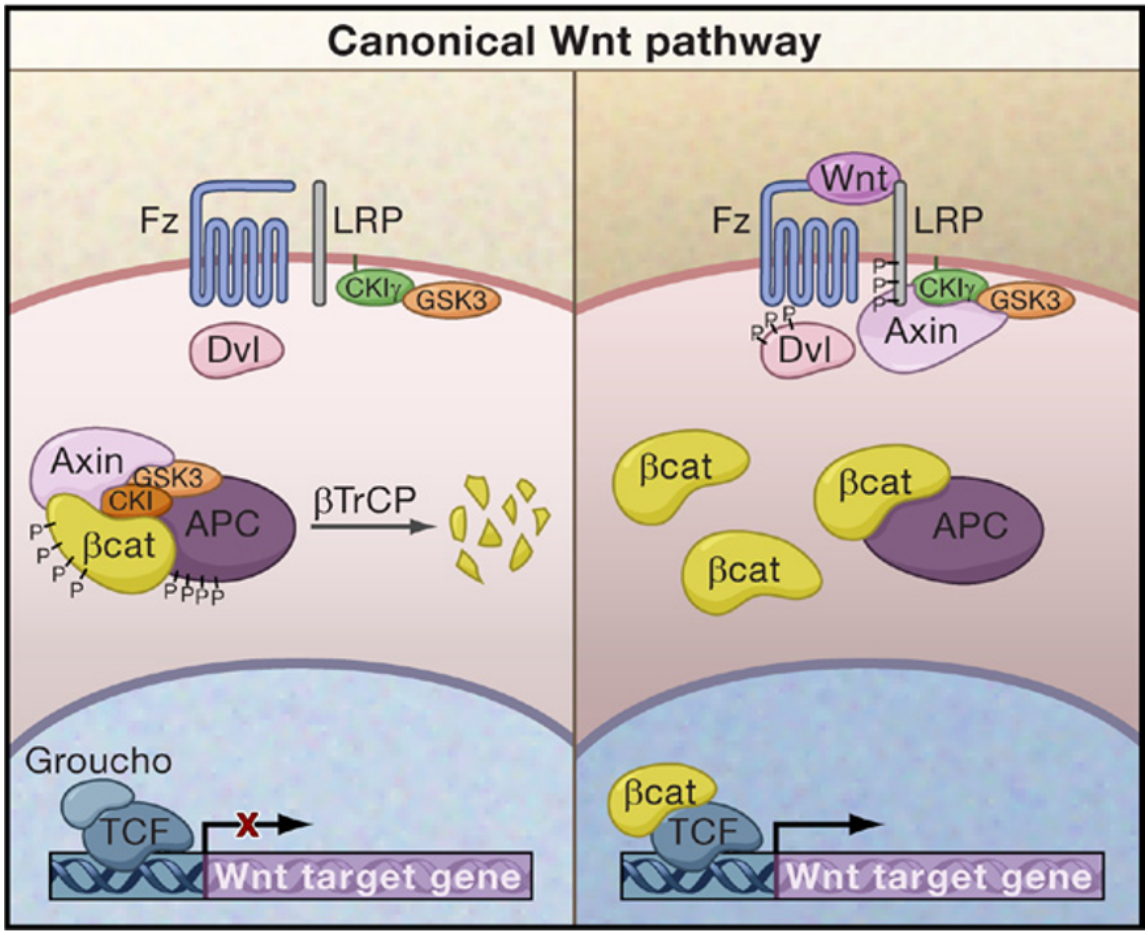

Figure 1.2. Canonical Wnt/β-catenin signaling pathway in its inactive (left) and active (right) states. (Adopted from Clevers, 2006)

β-catenin is not only the key signaling molecule in the canonical Wnt pathway but also functions in cytoskeleton as it binds to type I cadherins and α-catenin, forming adherent junctions between cells under resting conditions (Jamora & Fuchs, 2002). It links E-cadherin to α-catenin thereby regulating actin filament assembly by binding to the cytoplasmic domain of the E-cadherin. In the off state of Wnt signaling, CK1 phosphorylates β-catenin at serine 45 followed by phosphorylation by GSK3β, leading to its degradation (Lee, Kim, & Wands, 2006). In the on-state of Wnt signaling, β-catenin accumulates in the cytoplasm and is translocated into the nucleus where it interacts with the T cell factor/Lymphoid enhancer factor (TCF/LEF) family of transcription factors and activates the expression of target genes. Otherwise, the

TCF/LEF family of transcription factors recruit the co-repressor Groucho and inhibits target gene expression. β-catenin contains a core region composed of 12 copies of a motif called armadillo repeat which forms a superhelix of helices having a long, positively charged groove (Huber, Nelson, & Weis, 1997).

An important component of the β-catenin destruction complex is the serine/threonine kinase glycogen synthase kinase 3 beta (GSK3β). GSK3β phosphorylation of β-catenin is essential for inactivation of the Wnt pathway which takes place at serine 33, serine 37, and threonine 41 residues (Behrens *et al.*, 1998). Point mutations at these residues result in the stabilization of β-catenin as well as LiCl treatment to inactivate GSK3β, causing an overall increase in the Wnt signaling (Aberle *et al.*, 1997).

Axin, being the main scaffold protein of the destruction complex, contains separate binding sites for Dsh, APC, GSK3β, β-catenin, and PP2A. Axin mediates phosphorylation of β-catenin, APC, and Axin itself by GSK3β in the Wnt inactive status, whereas when Axin is recruited to the plasma membrane β-catenin phosphorylation by GSK3β is kept at a very low rate (Ikeda *et al*., 1998).

Adenomatous Polyposis Coli gene product (APC) is a tumor suppressor protein that has a series of 15 and 20 amino acid repeats through which it interacts with β-catenin. 20 amino acid repeats of APC is involved in downregulating β-catenin in the cell (Lee *et al*., 2006).

1.5. Wnt/β-catenin pathway and Cancer

Association of the Wnt/β-catenin signaling pathway deregulation with cancer has been well documented. There are both positively and negatively acting components, being activation of the components and loss of function mutations in tumor suppressors, respectively. Among the suppressing components of the Wnt pathway, particularly, APC tumor suppressor deficiency leading to constitutively activated Wnt/β-catenin signaling gives rise to excessive stem cell renewal and proliferation. APC mutations cause familial adenomatous polyposis and the vast

majority of all sporadic colorectal cancers (Polakis, 2012). Axin is also a tumor suppressor which found mutated in hepatocellular, colorectal, and in some familial cancer syndromes (Lammi *et al*., 2004; Marvin *et al.*, 2011; Salahshor & Woodgett, 2005). Inactivating mutations also comprises GSK3 genes, specifically in-frame splice deletion affecting the kinase domain of GSK3β found in chronic myelogenous leukemia (Abrahamsson *et al.*, 2009)

Mutations in the proto-oncogene β-catenin that prevents its phosphorylation and subsequent degradation are found in many cancers including hepatocellular carcinoma and medulloblastoma (Polakis, 2007). Additionally, aberrant splicing of co-receptor LRP5 that results in the deletion of the region interacting with the secreted Wnt signaling repressor DDK1 has also been described (Björklund *et al.*, 2009). Several cancers have also showed increased expression of Wnt ligands Qnt1, Wnt2, and Wnt7A during the development of glioblastoma, oesophageal cancer, and ovarian cancer, respectively (Anastas & Moon, 2013). Furthermore, aberrant activation of Wnt signaling-caused β-catenin accumulation in the nucleus has been observed in hepatocellular carcinoma, colorectal cancer, breast cancer, as well as gastrointestinal cancer. Studies on cancer so far indicate that hepatocellular carcinoma and colorectal carcinoma harbour the highest rate of Wnt signaling components mutations (Giles, Van Es, & Clevers, 2003).

1.5.1. The Role of Wnt/β-catenin Pathway in Hepatocellular Carcinoma

Nuclear and/or cellular accumulation of β-catenin has been observed in 33-67% of hepatocellular tumors, and has been found to correlate with tumor progression and poor prognosis (Lee *et al.,* 2006). Tumors exhibiting β-catenin accumulations were associated with high proliferative activity (Inagawa *et al.*, 2002), poorly differentiated morphology (Endo *et al.*, 2000), vascular invasion and dismal prognosis (Wong, Fan, & Ng, 2001). β-catenin mutations and accumulation show a significant correlation in HCC. Mutation in the exon 3 of the β-catenin gene is associated with increased tumor size and macrovascular/ microvascular invasion in HCC (Cieply *et al.*, 2009). However, many HCCs with β-catenin accumulation do not have APC or β-catenin mutations (Wong *et al.*, 2001), suggesting that other components of the signaling cascade may be important in the activation of canonical Wnt pathway during

hepatocarcinogenesis. Moreover, FZD7 was markedly increased in both transgenic mice of HCC and human hepatocellular tumors and may be an early event in hepatocarcinogenesis (Merle *et al.*, 2005). There are many more studies demonstrating mutations or deregulations of the Wnt pathway linking the cascade to HCC.

The canonical Wnt pathway plays a pivotal role in liver development, regeneration, and cancer. Accordingly, loss of β-catenin signaling leads to an increase in apoptosis, and knockdown of β-catenin culminates in decreased liver regeneration (Nejak-Bowen *et al.*, 2013)

1.6. Identification of novel targets of Wnt/β-catenin pathway

Identification of novel transcriptional targets of the Wnt/β-catenin pathway is an important step to the cancer research and finding potential targeted therapies; therefore, it is crucial to determine transcriptional targets whose expressions are regulated by this pathway.

Several different approaches have been utilized in order to identify novel targets of the Wnt/β-catenin signaling pathway. To do this, hepatocellular carcinoma derived Huh7 cells stably overexpressing a degradation-resistant, mutant form of β-catenin (S33Y) have been compared to control Huh7 cells. Transcriptome-profile analyses including SAGE (Serial Analysis of Gene Expression) and genome-wide microarray screens were performed to determine differential expression of potential target genes in response to pathway activation (Table 1.2). In addition, several experiments were carried out to further determine the novel molecules involved in the canonical Wnt pathway.

1.6.1. BRI3 as a novel Wnt/β-catenin pathway target gene

Among the candidate genes, BRI3 was found upregulated and confirmed to be one of the novel transccriptional targets of the Wnt/β-catenin signaling pathway by using lithium treatment of Huh7 cells, luciferase reporter assay, overexpression of Wnt ligands and chromatin immunoprecipitation (ChIP) assay (Kavak *et al.*, 2010). In addition, tumors bearing BRI3

overexpression showed higher proliferative and invasive characteristics compared to control (Akiva, 2016).

Table 1.2. Fold changes for the selected candidate genes with respect to Microarray, SAGE and qRT-PCR results. SAGE and Microarray folds are denoted as ratio of Huh7-S33Y-β-catenin/Huh7-vector (ND: non-detected) (Kavak *et al.,* 2010).

Gene	Microarray Fold	SAGE *p value*	SAGE Fold	qRT-PCR or RT-PCR Result
TINP1	0.97	0.46	-1.02	1.31
CLU	1.29	0.00	1.97	1.78
MGC40157	1.46	0.01	2.50	2.13
BRI3*	1.01*	0.01*	2.36*	2.99*
NES	0.81	0.00	-3.38	0.40
SEC31L1	0.89	0.00	-5.33	1.09
APOA2	0.78	0.00	-2.45	1.07
MGAT1*	1.17*	0.04*	3.00*	Up*
KIAA1924 (WDR90)	1.01	0.02	-6.00	Down
ATP5G1	0.78	0.00	-5.00	Down
TPT1	1.10	0.00	1.73	Up
BLP1 (tm2d2)	0.95	0.01	6.00	Up
MMP7nd	ND	ND	ND	No change
MYC	1.13	ND	ND	Up
HSF2	1.24	ND	ND	2.10 (α-isoform) 1.30 (β-isoform)

BRI3 (Brain protein 3) is a type II transmembrane protein with 267 amino acids that is overexpressed in TNF-α treated L929 murine fibrosarcoma cells (Wu *et al.*, 2003). It was shown to participate in TNF-α induced cell death based on the findings that using BRI3-antisense RNA resulted in 1000-fold increased resistance of L929 cells to apoptosis. Zhang and his colleagues recently discovered BRI3 promote cell proliferation and migration in DAOY cells. BRI3 was found upregulated in medulloblastoma cells and its overexpression activated the Wnt and p38/ERK/AKT pathways (Zhang, Wang, & Chen, 2017). Furthermore, BRI3 overexpression

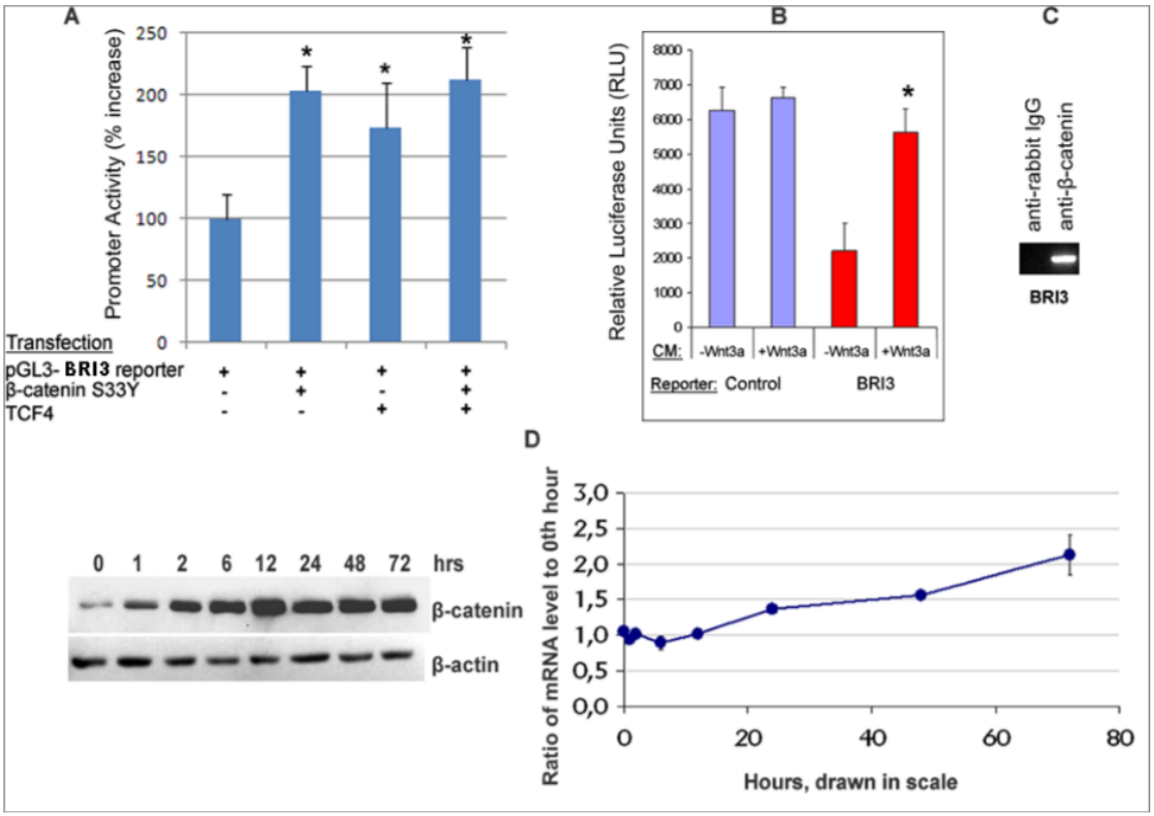

Figure 1.3. BRI3 was determined to be a novel target of Wnt/β-catenin signaling pathway by means of different approaches. (A) Luciferase reporter assay, (B), Wnt ligand overexpression, (C) CoIP and (D) Lithium treatment for β-catenin activation (Kavak *et al.*, 2010).

promoted the proliferation and migration of breast cancer cells and pancreatic neuroendocrine tumor cells via upregulating the p38/ERK/AKT and Wnt pathways (Guo *et al.*, 2014; Zhang & Feng, 2017).

In order to investigate the possible contribution of BRI3 in hepatocellular carcinogenesis, RNA-Seq analysis of tumors derived from BRI3 overexpressing Huh7 cells together with the corresponding control tumors derived from the GFP overexpressing cells was carried out. Based on having the highest fold change in the RNA-Seq analysis and relevance to cancer, three genes were chosen for further examination: YAP1, CSNK2β and AFP.

1.6.2. MGAT1 as a novel Wnt/β-catenin pathway target gene

Because SAGE and microarray screens also determined MGAT1 as upregulated under Wnt over-activation conditions, MGAT1 was too considered as a putative target of the Wnt/β-catenin signaling pathway and was confirmed to be upregulated by qRT-PCR, Western Blot, lithium chloride treatment, and luciferase reporter assay. Furthermore, wound healing assay and

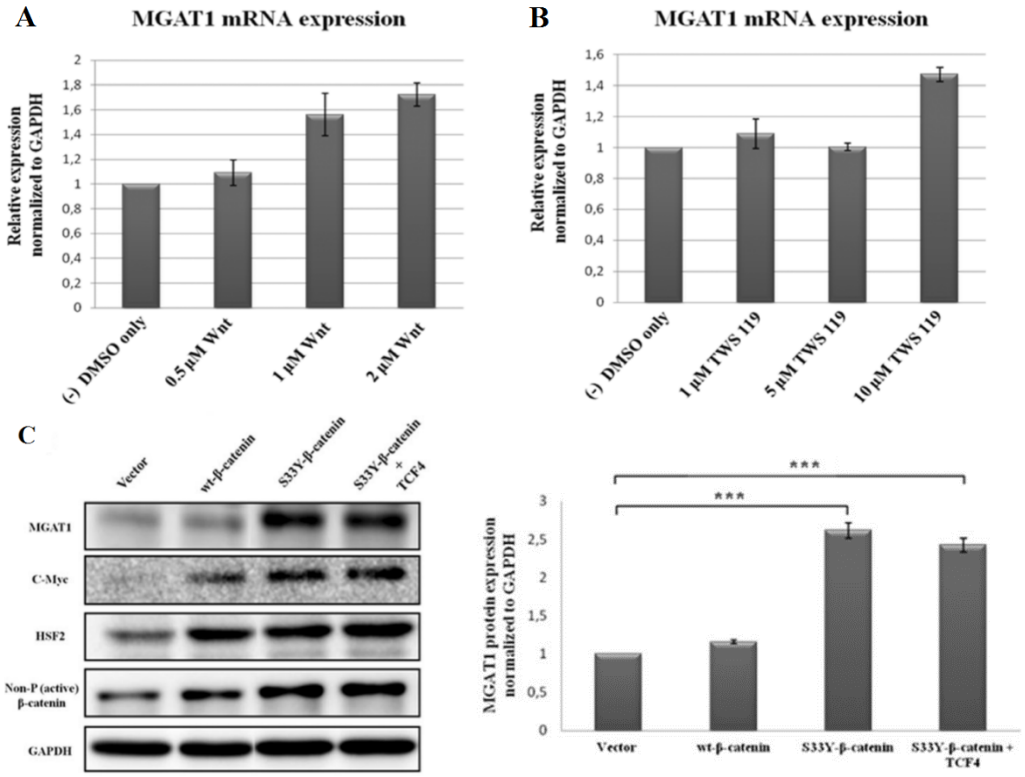

Figure 1.4. MGAT1 was determined to be a novel target of Wnt/β-catenin signaling pathway by means of different approaches. (A) qRT-PCR analysis in Huh7 cells treated with Wnt agonist, (B) and TWS 119, (C) Western blotting of Huh7 cells overexpressing of WT and S33Y-β-catenin (Akiva and İyison, 2018).

xenograft experiments showed that Huh7 cells stably overexpressing MGAT1 have more proliferative and invasive capabilities compared to control (Akiva & Birgül Iyison, 2018).

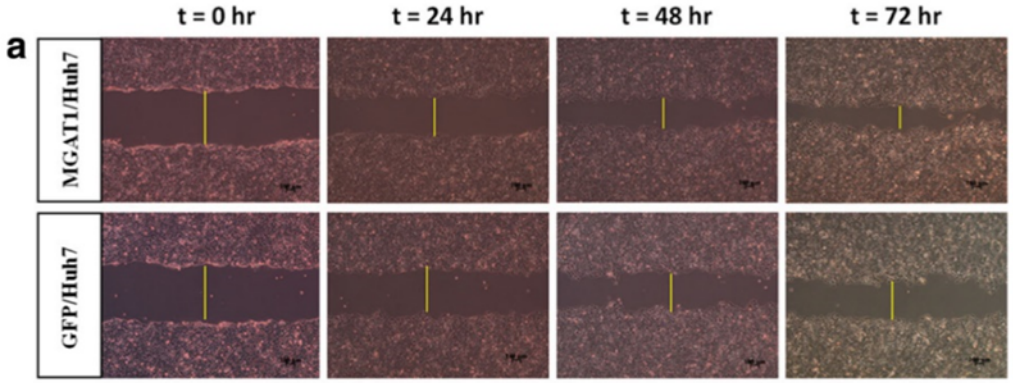

b

Stable cells	Percent wound closure
MGAT1/ Huh7	60,4 %
GFP/ Huh7	42,5 %

Figure 1.5. Wound healing assay for the stable Huh7 cells overexpressing either MGAT1 or GFP genes (Akiva and İyison, 2018).

MGAT1 (Mannosyl (alpha-1,3-)-glycoprotein beta-1,2-N-acetylglucosaminyl-transferase) is a type II transmembrane protein with 445 amino acids which is a medial Golgi enzyme catalyzing the first step in the conversion of oligomannose-type N-glycans into complex and hybrid N-glycans (Yip *et al.*, 1997). Previous studies showed that lacking functional MGAT1 gene resulted in death at approximately 10 days after fertilization, suggesting that MGAT1-dependent N-glycans are essential for cell-cell interactions (Ioffe, Liu, & Stanley, 1997). To investigate the potential role of MGAT1 in cancer, a group of researchers carried out knockdown experiments. shRNA knockdown of MGAT1 in HeLa cervical tumor cells inhibited cell migration and invasion. *In vivo*, PC-3-Yellow orthopic prostate cancer xenograft model showed a significant decrease in primary tumor growth under MGAT1 shRNA treatment (Beheshti Zavareh *et al.*, 2012).

To investigate the possible role of MGAT1 in tumorigenesis of hepatocytes, tumors derived from either GFP or MGAT1 overexpressing Huh7 cells were subjected to RNA-Seq analysis. Based on having the highest fold change and their relevance to cancer, three genes were selected for further examination: EDNRB, ADAM17 and HSPA8.

1.7. Hippo Pathway

The size of developing organs and tissue homeostasis are controlled by cell growth, proliferation and apoptosis, which collectively regulate cell size and cell numbers (Conlon & Raff, 1999). Hippo pathway is one of the many signaling pathways that control these cellular processes. Components of the Hippo pathway are evolutionary conserved, and inactivation of this signaling cascade is involved in cancer as it is required to restrict cell growth and proliferation, as well as to induce cell death.

The Hippo pathway components were first discovered in *Droshophila* in search of genes regulating the growth of larval tissues and many of them were classified as tumor suppressors except the transcriptional coactivators YAP/TAZ (Genevet & Tapon, 2011; Halder & Johnson, 2011; Justice *et al.*, 1995). *Droshophila* core Hippo pathway components have direct homologs in mammals. The core Hippo kinase cascade in mammals starts with MST1/2 kinases binding to their regulatory protein SAV1 to form an active enzyme, which in turn phosphorylate LATS1/2 kinases (Chan *et al.*, 2005). MST1/2 kinases also phosphorylate the MOB1A/B regulatory subunits of LATS1/2 (Praskova, Xia, & Avruch, 2008). Activation of the LATS1/2-MOB1A/B complex then phosphorylates YAP/TAZ, the two main effectors of the Hippo pathway (Dong *et al.*, 2007; Lei *et al.*, 2008; Zhao *et al.*, 2007). YAP/TAZ phosphorylation inhibits their activity and the mechanisms providing this process are nuclear exclusion, sequestration in the cytoplasm, and/or proteolytic degradation by proteasomes (Liu *et al.*, 2010; Zhao *et al.*, 2010; Zhao *et al.*, 2007). YAP phosphorylation by LATS1/2 at S127 in general leads to sequestration of YAP in the cytoplasm but in some cases, S127-phosphorylated YAP by a kinase other than LATS1/2 is found in the nucleus (Wada *et al.*, 2011). Merlin is an important inhibitor of YAP/TAZ complex encoded by the NF2 (neurofibromatosis type 2) tumor

suppressor gene. It acts upstream of the Hippo kinases, and mutations in this gene lead to tumors of the nervous system (Gusella *et al.*, 1999).

Until recently, the main regulatory input upstream YAP/TAZ has been regarded as the Hippo cascade but now Wnt and GPCR signaling pathways are also recognized as regulators of YAP/TAZ activity (Azzolin *et al.*, 2012; F. X. Yu *et al.*, 2012). YAP 127 phosphorylation is a target of AKT, and in the liver S127 phosphorylation may occur independent of LATS1/2 (Basu *et al.*, 2004; Zhou *et al.,* 2017). Moreover, mechanical signals also pass on information to individual cells about their shape and structural properties of their microenvironment that act as local and organ-level checkpoints regulating YAP/TAZ activity, but the mechanism is still unclear.

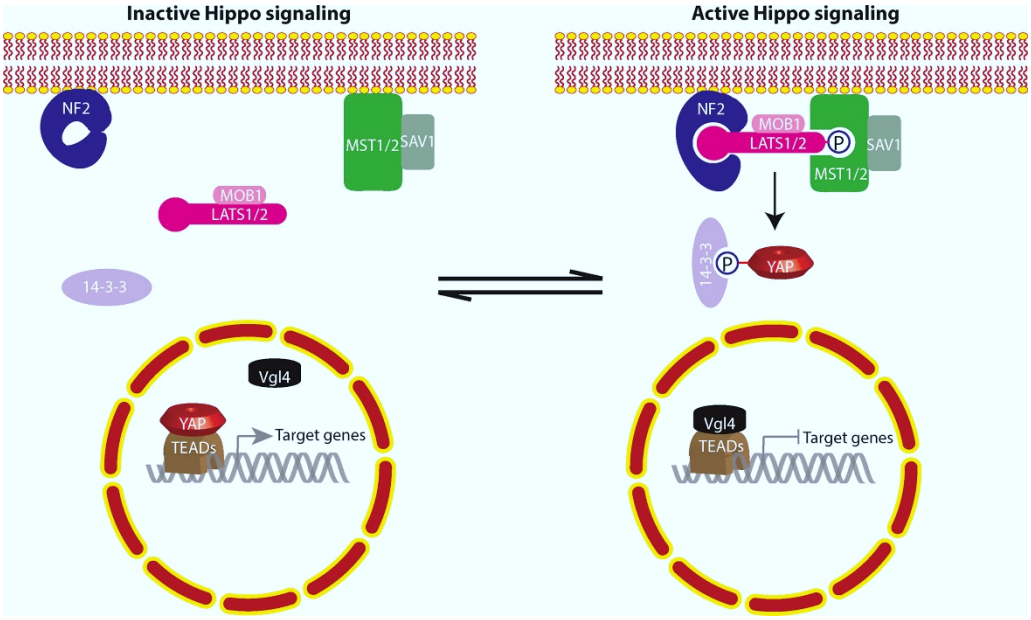

Figure 1.6. The mammalian Hippo pathway in its inactive (left) and active (right) states. (Adopted from Piccolo, Dupont, & Cordenonsi, 2014)

1.7.1. Hippo pathway regulation by multiple inputs

Multiple inputs modulate the Hippo pathway in a coordinated or independent fashion. YAP phosphorylation by LATS1/2 inhibits YAP/TAZ transcriptional coactivators by spatial separation from binding to their nuclear target transcriptional factors including TEAD family members (Zhao *et al.*, 2008). There are several different mechanisms other than LATS1/2 phosphorylation that regulates YAP/TAZ activity. Density-dependent activation of the Hippo pathway and subsequent increase in YAP phosphorylation was previously reported by Zhao and his colleagues (Zhao *et al.*, 2007). Also, changes in cell morphology are key aspect; and F-actin controlled YAP activity downstream of cell morphology, independent from cell-cell contact or adhesion (Wada *et al*., 2011). Cells detect density through their morphology and modulates YAP/TAZ activity via stress-fibers, and this pathway probably cooperates with a cell contact-mediated mechanism to accomplish density-dependent regulation of cell proliferation.

Oncogenic stress signal Ras was shown to induce MST1 activity that result in apoptosis (Khokhlatchev *et al.*, 2002). Epinephrine or glucagon stimulation of Gs-coupled receptors increases LATS1/2 kinase activity and activates the Hippo pathway (Yu *et al.*, 2012). Several other inputs such as DNA damage (Hamilton *et al.*, 2009), a cell surface hyaluronan receptor CD44 (Xu, Stamenkovic, & Yu, 2010), and F-actin depolymerization (Densham *et al.*, 2009) have also been reported to feed into the Hippo pathway.

1.8. YAP/TAZ and Cancer

YAP/TAZ biological properties are often used to foster proliferation, migration, invasion, and metastasis in human tumors. YAP protein has been detected in many cancers including late-stage ovarian, colon, liver, gastric, non-small-lung, esophageal, and invasive breast cancers; in line, high expression of YAP/TAZ target genes are associated with poor outcome in large datasets of colon and breast cancer patients (Piccolo *et al.*, 2014).

Hippo-regulated YAP/TAZ is involved in loss of control over proliferation. Overexpression of mutant nonphosphorylatable YAP or TAZ increases proliferation in several

human cell lines *in vitro* (Lei *et al*., 2008; Ota & Sasaki, 2008; Zhao *et al.*, 2008). Conversely, YAP/TAZ depletion by RNA interference halts growth of various human cancer cells (Azzolin *et al.*, 2012; Siew *et al.*, 2008).

Loss of cell substrate contacts (anoikis)-induced cancer cell death is repressed by YAP and TAZ (Zhao *et al.*, 2012). Contrarily, Yuan and his colleagues showed that YAP1 knockdown rendered BT474 and MDA-MB-231 breast cancer cells significantly resistant to anoikis, suggesting that YAP1 functions as a tumor suppressor in breast. YAP suppressed breast cancer cells exhibit enhanced migration and invasion capabilities (Yuan *et al.*, 2008). YAP might function as an oncogene and tumor suppressor in a context-dependent manner, a phenomena already proven in other studies (Rowland & Peeper, 2006).

Mutations in the components of Hippo pathway are extremely rare in human cancers except for NF2. This suggests that the Hippo pathway may be targeted nongenetically in the course of tumorigenesis, commonly by disturbed cell polarity or EMT (Azzolin *et al.*, 2012). Aberrant pro-YAP/TAZ mechanical signals blends with epigenetic inactivation of Hippo to disrupt tumor suppressor properties of healthy tissues (Egeblad, Rasch, & Weaver, 2010).

1.9. Crosstalk between YAP/TAZ and Wnt signaling

Azzolin and his colleagues demonstrated YAP/TAZ as components of the β-catenin destruction complex (Azzolin *et al*., 2014). YAP/TAZ bind to Axin and are required for β-TrCP recruitment to the complex. Therefore, YAP/TAZ are critical for β-catenin degradation in Wnt off-state, and absence of YAP/TAZ causes activation of β-catenin/TCF transcriptional responses. Upon Wnt ligand binding, YAP/TAZ are released from the destruction complex; making β-catenin invisible to β-TrCP and leading to β-catenin accumulation in the cytolasm as well as sequestering YAP/TAZ in the nucleus and leading to YAP/TAZ-dependent transcriptional responses (Azzolin *et al.*, 2014). Independent of its kinase function, LATS1/2 has been linked to inactivation of Wnt/β-catenin signaling by interfering β-catenin interacting with its essential cofactor BCL9 (J. Li et al., 2013). Collectively, the data brings two distinct

scenarios into mind: cytoplasmic retention of YAP/TAZ complex (Hippo on-state) bar Wnt/β-catenin signaling; conversely a Hippo off-state would warrant activation of both Wnt/β-catenin and Wnt/YAP/TAZ signaling pathways Figure 1.3.

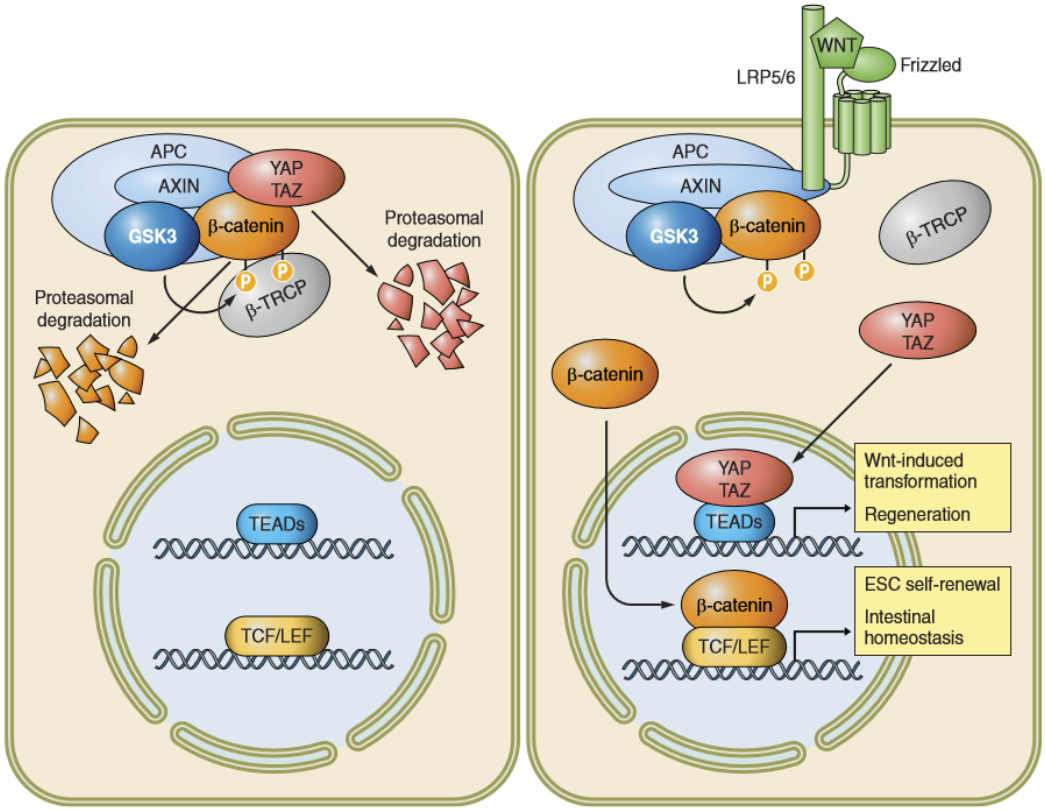

Figure 1.7. Role of YAP/TAZ in Wnt signaling (Adopted from Azzolin *et al.*, 2014).

2. AIM OF THE STUDY

Wnt/β-catenin pathway is one of the most fundamental signaling pathway in vertebrates which controls embryonic development and adult homeostasis. Mutations in the components of this pathway are identified to have a tumorigenic effect, and genes regulated by this pathway are potential drug and gene therapy targets. Therefore, it is a key step to identify and characterize novel targets of the Wnt/β-catenin pathway to shed light into the complex signaling in tumorigenesis.

In this study, the main objective was to validate differential expressions of selected genes in either BRI3 or MGAT1 overexpressing cells in order to elucidate the roles and ultimate implications of these novel target genes of Wnt/β-catenin pathway in hepatocellular cancer. We performed a number of experiments to check the mRNA and protein levels of selected genes in control and BRI3 or MGAT1 overexpressing cells. To further investigate the involvement of BRI3 and MGAT1 genes in hepatocellular carcinoma, we searched for links between the selected genes of BRI3 and MGAT1 separately by literature research. Using a bioinformatic tool that provides prediction of direct protein-protein interactions, we were able to detect physical interactions in different combinations of the selected genes. Collectively, these results provide further information of the underlying mechanism leading to hepatocellular carcinogenesis.

3. MATERIALS

3.1. General Kits, Enzymes and Reagents

Table 3.1. List of kits, enzymes and reagents.

Name	**Supplier**
BCA Protein Assay Kit	Thermo, USA
Fetal Bovine Serum (FBS)	Gibco, USA
Protein Molecular Weight Marker	PageRuler Prestained Protein Ladder, Thermo, USA
Complete Mini PI (Protease Inhibitor)	Roche, Switzerland
Taq DNA polymerase	Thermo, USA
Phusion High-Fidelity DNA polymerase	NEB, USA
Dulbecco's Modified Eagle Medium (DMEM)	Hyclone, USA
DNA Molecular Weight Marker	GeneRuler 1 kb DNA Ladder, Fermentas, USA
NucleoBond Xtra Plasmid Midiprep Kit	Macherey-Nagel, Germany
Direct-Zol RNA Miniprep Kit	Zymo, USA
High Pure RNA Isolation kit	Roche, Switzerland
SensiFast cDNA Synthesis Kit	Boline, UK
SensiFast SYBR No-Rox Kit	Bioline, UK
Penicillin/Streptomycin (10X)	Hyclone, USA
Turbofect Transfection Reagent	Thermo, USA
Lipofectamine 2000 Transfection Reagent	Thermo, USA
Rnase A	Roche, Switzerlan0d

Table 3.1. List of kits, enzymes and reagents (cont.).

Name	Supplier
Trypsin-EDTA (0.5 mM EDTA, 0.0025% Trypsin)	Hyclone, USA
WesternBright ECL HRP substrate	Advansta, USA

3.2. Biological Materials

3.2.1. Mammalian Cell Lines

Huh7 human hepatocellular carcinoma cell line was kindly provided by Dr. Mehmet Öztürk and used in this study.

3.3. Buffers and Solutions

3.3.1. DNA Gel Electrophoresis

Table 3.3. DNA gel electrophoresis buffers and solutions.

Solution/Buffer	Content
X Tris-acetic acid EDTA (TAE)	2M Tris-acetate 50mM EDTA pH 8.5
TE Buffer	10mM Tris–HCl 1mM EDTA pH 8.0

Table 3.3. DNA gel electrophoresis buffers and solutions.

Ethidium bromide (EtBr)	10 mg/ml (stock solution) 30 ng/ml (working solution)
10X Tris Borate EDTA (TBE)	108 g Tris base 55 g Boric acid 9.3 g EDTA Double distilled water up to 1 L
6X Loading Buffer	2.4 ml dH2O 0.1 ml 1M Tris-HCl pH 7.6 0.3 ml 1% Bromophenol Blue (BPB) 6 ml 100 per cent glycerol 1.2 ml 0.5M EDTA distilled water up to 10 ml

3.3.2. RNA Gel Electrophoresis

Table 3.4. RNA Gel Electrophoresis buffers and solutions.

Solution/Buffer	**Content**
Diethylpyrocarbonate treated water	1% (v/v) Diethylpyrocarbonate
10X Morpholino Propane Sulfonic Acid (MOPS)	41.8 g MOPS 20ml 0.5M EDTA 16.8ml 3M NaOAc DEPC treated water upto 1L pH 7.00
EtBr RNA loading buffer	0.72 ml formamide 0.16 ml 10X MOPS 0.26 ml formaldehyde 0.18 ml DEPC treated water 0.1 ml 80% Glycerol 0.08 ml Bromophenol blue 50 µg EtBr

3.3.3. Western Blotting Buffers and Solutions

Table 3.5. SDS-PAGE and Western Blotting buffers and solutions.

Solution/Buffer	**Content**
12% SDS-PAGE gel (separating gel)	12% Acrylamide : Bisacrylamide (37.5:1) 375mM Tris-HCl (pH 8.8) 0.1%SDS 0.1% APS 0.1% TEMED
6 % SDS- PAGE gel (stacking gel)	6% Acrylamide : Bisacrylamide (37.5:1) 125mM Tris-HCl (pH 6.8) 0.1% SDS 0.1% APS 0.1% TEMED
5X SDS-PAGE Loading Dye	250 mM Tris-HCl (pH 6.8) 10% SDS 50% Glycerol 5% β-mercaptoethanol 0.1% Bromophenolblue
10X SDS Running Buffer	30.3 g Tris base 144.4 g Glycine 10 g SDS distilled water up to 1 L
10X Transfer Buffer	30.3 g Tris base 144.4 g Glycine distilled water up to 1 L
1X Transfer Buffer	100 ml 10X Transfer Buffer 200 ml Methanol 700 ml distilled water
10X TBS (Tris Buffered Saline)	24.23 g Tris Base 80.06 g NaCl distilled water up to 1 L pH 7.4 - 7.6
6 % SDS- PAGE gel (stacking gel)	6% Acrylamide : Bisacrylamide (37.5:1) 125mM Tris-HCl (pH 6.8) 0.1% SDS 0.1% APS 0.1% TEMED

Table 3.5. SDS-PAGE and Western Blotting buffers and solutions (cont.).

Solution/Buffer	**Content**
5X SDS-PAGE Loading Dye	250 mM Tris-HCl (pH 6.8) 10% SDS 50% Glycerol 5% β-mercaptoethanol 0.1% Bromophenolblue
10X SDS Running Buffer	30.3 g Tris base 144.4 g Glycine 10 g SDS distilled water up to 1 L
10X Transfer Buffer	30.3 g Tris base 144.4 g Glycine distilled water up to 1 L
1X Transfer Buffer	100 ml 10X Transfer Buffer 200 ml Methanol 700 ml distilled water

Table 3.5. SDS-PAGE and Western Blotting buffers and solutions (cont.).

1X TBST (Tris Buffered Saline with Tween-20)	100 ml 10X TBST 900 ml distilled water 10 ml 10% Tween-20
Blocking Solution	3% BSA powder 1X TBS-T
Stripping Solution	62.5 mM Tris-HCl 2% SDS 0.7% β-mercaptoethanol pH 6.8

3.3.4. Polymerase Chain Reaction

Table 3. 6. Polymerase chain reaction buffers and solutions.

Solution/Buffer	**Content**
5X HA Buffer	Promega, USA

Table 3. 6. Polymerase chain reaction buffers and solutions (cont.).

Solution/Buffer	**Content**
Dimethylsulphoxide (DMSO)	Applichem, Germany
Deoxyribonucleotides (dNTPs)	100 mM of each dNTP

3.3.5. Bacterial Culture Solutions and Antibiotics

Table 3. 7. Solutions and Antibiotics used for the growth and maintenance of bacterial cultures.

Solution/Buffer	**Content**
Luria-Bertani medium (LB)	10 g tryptophan 5 g yeast extract 10 g NaCl Distilled water up to 1 L, autoclaved
Ampicillin stock	100 mg/ml in 50 % Ethanol Filter-sterilized and stored at -20°C 100 µg/ml (working concentration)
Kanamycin stock	50 mg/ml in distilled water Filter-sterilized and stored at -20°C 50 µg/ml (working concentration)

3.4. Nucleic Acids

DNA molecular weight markers and deoxyribonucleotides were purchased from Fermentas (USA).

3.4.1. Plasmids

pEGFP-N2 (Clontech, CA, USA), PGL3 (Promega, Wisconsin, USA), pIRES2-EGFP (Clontech, CA, USA) plasmids were commercially obtained. PGL3-GFP, pEGFP-N2-BRI3 and MGAT1-pIRES2-EGFP plasmids were kindly provided by Dr. İzzet Akiva, Boğaziçi University.

3.4.2. Oligonucleotides

Primers used in sequencing and polymerase chain reactions were purchased from Macrogen Inc. (Seoul, South Korea). Lyophilized oligonucleotides were dissolved in dH_2O to have a final concentration of 100 pmol/µL Sequences of the primers used in this study are shown in Table 3.8.

Table 3.8. Primers used for qRT-PCR.

Primer ID	**Sequence**
YAP1-F	TAGCCCTGCGTAGCCAGTTA
YAP1-R	TCATGCTTAGTCCACTGTCTGT
CSNK2β-F	TCCTGGATTTCCTGGTTCTG
CSNK2β-R	CACTCTGGTTGGGGTTGTCT
AFP-F	CAGCCACTTGTTGCCAACTC
AFP-R	GCAGCATTTCTCCAACAGGC
GAPDH-F	TGTGGCCATCAATGGATTTGG
GAPDH-R	ACACCATGTATTCCGGGTCAA
EDNRB-F	GTCCCAATATCTTGATCGCAG
EDNRB-R	AAGGCACCAGCTTACACATCT
ADAM17-F	GACTCTAGGGTTCTAGCCCAC
ADAM17-R	GGAGACTGCAAACGTGAAACAT
HSPA8-F	ACCTACTCTTGTGTGGGTGTT
HSPA8-R	GACATAGCTTGGAGTGGTTCG

3.5. Antibodies

Table 3.9. Antibodies used throughout this study.

Antigen	**Supplier**	**Host**	**MW(kDa)**
YAP1	Abnova	Rabbit	80
AFP	R&D	Mouse	75
CSNK2β	Santa Cruz	Mouse	28
B-Actin	Cell Signaling	Rabbit	47
EDNRB	Fitzgerald	Rabbit	67
HSPA8	Cell Signaling	Rabbit	72
ADAM17	Abcam	Rabbit	80

3.6. Disposable Labware

Table 3. 10. List of disposable labware used in this study.

Cell Culture Plates (10 cm, 6 cm 6-well, 96-well)	VWR, USA
Centrifuge Tubes (15 ml, 50 ml)	VWR, USA
Microfuge Tubes (1.5 ml, 2 ml)	Axygen, USA
PCR Tubes (0.2 ml)	Axygen, USA
Cryovial Tubes	Grenier Bio One, UK
Western Blotting Paper	Whatmann, UK
Serological Pipettes (5 ml, 10 ml, 25 ml)	Capp, Denmark

Pipette Tips (Bulk)	Axygen, USA
Pipette Tips (Filtered)	CAPP, Denmark
96-well plates for qRT-PCR	Roche, Switzerland
96-well plates for qRT-PCR	Bioplastics, Netherlands
Insulin syringes (1 ml)	Set Medikal, Turkey
Serological Pipettes (5 ml, 10 ml, 25 ml)	Capp, Denmark
Cell Scraper	TPP, Switzerland
96-well plates for qRT-PCR	Bioplastics, Netherlands

3.7. General Equipment

Table 3. 11. Equipment used in this study.

Equipment	**Supplier**
Agarose Gel Electrophoresis System	Mini-sub Cell GT, BioRad, USA
Autoclaves	MAC-601, Eyela, Japan ASB260T, Astell, UK
Balances	Electronic Balance VA 124, Gec Avery, UK DTBH 210, Sartorius, GERMANY
Carbon dioxide tank	2091, Habaş, TURKEY
Centrifuges	Centrifuge 5415R, Eppendorf, USA Allegra X22-R, Beckman, USA J2-21 Centrifuge, Beckman, USA J2-MC Centrifuge, Beckman, USA Mini Centrifuge 17307-05, Cole Parmer, USA
Cold room	Birikim Elektrik Soğutma, Turkey

Table 3. 11. Equipment used in this study (cont.).

Equipment	**Supplier**
Deep freezers	−20°C, 2021D, Arçelik, Turkey −70°C Freezer, Harris, UK −86°C ULT Freezer, ThermoForma, USA −152°C, MDF-1156, Sanyo, Japan
Documentation System	Gel Doc XR System, Bio-Doc, ITALY Stella, Raytest, Germany G:BOX Chemi XX6, Syngene, UK
Electrophoresis Equipments	Mini-Protean III Cell, Bio-Rad, USA
Heat blocks	DRI-Block DB-2A, Techne, UK
Hemocytometer	Improved Neubauer, Weber Scientific International Ltd. UK
Ice Machine	Scotsman Inc., AF20, ITALY
Incubator	Hepa Class II Forma Series, Thermo, USA
Laboratory Bottles	Isolab, GERMANY
Laminar flow cabinet	Labcaire BH18, UK
Liquid Nitrogen Tank	Air Liquide, TR21, FRANCE
Magnetic stirrer	Witeg, MSH-20D, GERMANY
Micropipettes	Eppendorf, GERMANY
Microplate Readers	680, Biorad, USA
Microscopes	Inverted Microscope, Axio Observer Z1, Zeiss, USA Light Microscope, CKX41, Olympus, JAPAN
Microwave oven	Philips Whirlpool, USA
pH meter	WTW pH330i, GERMANY

Table 3. 11. Equipment used in this study (cont.).

Equipment	**Supplier**
Pipettor	CAPP Controller, DENMARK
Power Supplies	Power Pac Universal, Biorad, USA EC135-90, Thermo Electron Corp,USA
Refrigerators	2082C, Arçelik, TURKEY 4030T, Arçelik, TURKEY
Scales	Precisa XT4200C, Germany
Shakers	VIB Orbital Shaker, InterMed, DENMARK Lab-Line Universal Oscillating Shaker, USA Thermo EC, Forma Orbital Shaker 420, USA
Pipettor	CAPP Controller, DENMARK
Power Supplies	Power Pac Universal, Biorad, USA EC135-90, Thermo Electron Corp,USA
Refrigerators	2082C, Arçelik, TURKEY 4030T, Arçelik, TURKEY
Softwares	Quantity One, Bio-Rad, ITALY ImageJ, Image Analysis Software, NIH, USA XStella 1.0, Stella, GERMANY
Spectrophotometer	Agilent 8453, USA NanoDrop ND-1000, Thermo, USA
Speed Vacuum	Thermo EC, SPD111V, USA
Thermocyclers	GeneAmp PCR System 2700, Applied Biosystems, USA
Vacuum pump	KNF Neuberger, USA
Vortex	Vortexmixer VM20, Chiltern Scientific, UK
Water baths	TE-10A, Techne, UK

4. METHODS

4.1. Plasmid Isolation

Previously prepared and verified MGAT1-pIRES2-EGFP, PGL3-GFP AND Pegfp-n2-brı3 containing bacterial stock (Akiva, 2016) were grown overnight in LB medium containing ampicillin or kanamycin at 37°C with shaking at 225 rpm. Isolation of the plasmids was performed by using MidiPrep kit (Qiagen, USA) as instructed by the manufacturer. First, cells were lysed and cleaned from chromosomal DNA by denaturing it under strong alkaline conditions. Cell debris was removed by centrifugation at 10.000 g for 10 minutes. Supernatant was applied to the QIAprep spin columns in which DNA binding to the silica membrane and removal of impurities by washing with wash buffer containing ethanol occur. Then, the plasmid DNA was eluted with dH_2O, and the concentrations and purity were ascertained by measuring optical density at 260 nm wavelength with the NanoDrop Spectrophotometer. Plasmids were stored at -20°C for later use.

4.2. Cell Culture

4.2.1. Maintenance of Huh7 Cells

Human hepatocellular carcinoma derived cell line Huh7 was grown in DMEM containing 10 per cent FBS (Gibco) and 1 per cent penicillin/streptomycin (Hyclone) in an incubator at 37ºC, with 5 per cent CO2 and 95 per cent air. DMEM media were stored at 4ºC and warmed to 37ºC in a water bath before use. Cells were passaged every 2-3 days before reaching ~90 per cent confluence. The growth medium was aspirated and the cells were washed once with 1X calcium and magnesium-free PBS. To remove the monolayer cells from the surface, the cells were treated with trypsin-EDTA solution (0.025 per cent trypsin, 0.5mM EDTA) and incubated at 37ºC for 3 minutes. 3 volumes of fresh medium were added for

inactivation of trypsin, suspended cells were transferred to a 15 ml falcon tube for centrifugation purposes at 1600 rpm for 2 minutes. The supernatant was aspirated and cell pellet was suspended in 4 ml of fresh growth medium. The cells were transferred evenly to sterile cell culture dishes containing growth medium in 1:4 ratio for standard passaging.

4.2.2. Cell Freezing

Stock solutions were prepared until further usage. Huh7 cells from 10 cm cell culture with ~80% confluency was frozen as stock solutions. The medium in the plates were aspirated and monolayer cells were washed with 1X PBS. 2 ml of trypsin was added onto the cells and incubated at 37ºC for 3 minutes. To inactivate the trypsin, 6 ml fresh medium was added, and the cell suspension was collected in a 15 ml falcon tube. The cells were then centrifuged at 1600 rpm for 2 minutes and the suspension medium was aspirated. Next, cell pellet was resuspended in 900 µ of fresh medium and 100 µl DMSO was added to have a final concentration of 10%. The cell suspension was evenly distributed into 2 ml cryogenic vials on ice and stored in isopropanol boxes at -80ºC for 2 days and transferred into -150ºC fridge until further usage.

4.2.3. Cell Thawing

Frozen cryogenic vials containing Huh7 cells were thawed in a 37ºC water bath for 1 minute and immediately mixed with 5 ml of fresh medium. Cell suspensions were then centrifuged at 1600 rpm for 2 minutes. Next, the cell pellet was resuspended in 1 ml of fresh medium and transferred to 10 cm culture dish containing 9 ml of fresh medium.

4.2.4. Transfection of Huh7 Cell Line

In the first part of this study, Turbofect transfection reagent (Thermo Scientific Inc., USA) was used according to DNA: reagent ratios suggested by the manufacturer to carry out transfection in mammalian cells. Pure DMEM without any FBS or antibiotics was used to make transfection complex and the solution was incubated at room temperature for 20 minutes. Then, the solution was added drop by drop onto the cells, assuring even distribution on 6-well plates.

After incubation of cells with transfection complex at 37 °C for 6 hours, medium change was performed. The cells were collected after 48-72 hours of transfection.

In the continuation of the study, transfection was carried out by using Lipofectamine 2000 transfection reagent (Thermo Scientific Inc., USA) according to DNA:reagent ratios suggested by the manufacturer. Transfection was done in 6-well plates when the cells were at ~90% confluency. Dilution of DNA and Lipofectamine 2000 reagent was carried out separately in 150 µl of pure DMEM per well. Then, 250 µl of DNA-lipid complex was first incubated for 5 minutes at room temperature and added onto the attached cells drop by drop, assuring even distribution. The cells were collected after 48-72 hours of transfection.

4.1. SDS-PAGE and Western Blotting

4.1.1. Cell Lysis and Protein Extraction from Huh7 Cell Line

Cell lysis and protein extraction was performed from cells in 6-well plates. The cells were first washed once with 1X PBS. Next, 150 ul of RIPA buffer containing protease inhibitors was added onto plates placed on ice. The plates were incubated for 30 minutes on ice and cells were then scraped using cell scrapers and collected into 1.5 ml eppendorf tubes. Obtained cell lysates were centrifuged at 12000g for 10 minutes at 4°C and supernatants were collected in new 1.5 ml eppendorf tubes. Protein lysates were stored at -20°C for short term storage or -80°C for long term storage.

4.1.2. Quantification of Protein Lysates

BCA Protein Assay Kit (Thermo Scientific Inc., USA) was used for quantification of protein lysates. Dilutions of bovine serum albumin (BSA) and unknown samples ranging from 0.025 to 2 mg/ml were prepared in a 96-well plate. 50:1 ratio of Reagent A:Reagent B was mixed to prepare BCA Working Reagent. 200 µl of BCA Working Reagent per well was prepared and added onto a 96-well plate on ice. Protein samples and BSA standards were added onto each well as 5 µl. The plate was covered with aluminum oil and incubated at 37°C for 30

minutes, then cooled down to room temperature. Absorbance measured at 562 using Plate Reader (VersaMax, Molecular Devices, USA). Concentrations of the protein samples were extrapolated using the standard curve.

4.1.3. SDS-PAGE

12% separating gels with 37:5:1 acrylamide: bis-acrylamide ratio was cast by using a Mini-Protean Tetra cell (BioRad) throughout the study. Isopropanol was added on top of the separating gel until the end of polymerization reaction to avoid any bubbles as well as to maintain a straight line. After polymerization was done, isopropanol was removed and 6% stacking gel with 37:5:1 acrylamide: bis-acrylamide ratio was prepared and quickly added on top of separating gel. 10-well comb was inserted at the top and kept there until usage. Polymerization reaction for stacking gel was waited for 15 minutes.

Tablo 4.1. Reagents used to prepare 2 mini SDS/PAGE gels.

	Separating Gel(12%)	**Stacking Gel(6%)**
Total Volume	16 ml	10 ml
ddH_2O	6.8 ml	5.2 ml
1.5M Tris-Cl (pH:8.8)	4 ml	-
1M Tris-Cl (pH:6.8)	-	2.5 ml
Acrylamide:Bisacrylamide (30% / 0.8% w/v)	6.4 ml	2 ml
SDS (10% w/v)	160 µl	100 µl
APS (10% w/v)	160 µl	100 µl
TEMED	16 µl	10 µl

4.1.4. Western Blotting

First, 5X SDS-PAGE loading dye was added to samples according to their volumes. 30-50 µg of protein was calculated to load into each well. Denaturation of proteins was performed by boiling the samples at 95°C for 5 minutes. Samples were then incubated on ice for 5 minutes before loading. After the removal of the comb from stacking gel in running buffer, the samples were loaded in order. As molecular weight standard, 5 µl of pre-stained protein marker (Thermo) was loaded into the first well. The gels were run in 1X running buffer at 80V until the BPB front reached separating gel and then voltage was increased to 120V. Running was completed when the BPB front left the separating gel. After, the glasses were removed carefully, stacking gels were also removed. The gels were equilibrated in 1X in transfer buffer for 10 minutes. Activation of PVDF membrane was done in methanol for 2 minutes then the membranes were placed in ddH_2O. Transfer cassettes were prepared, and membranes were placed onto the gels for transfer of proteins onto the membrane. Transfer process was carried out with 1X cold transfer buffer for 100 minutes at 100V in the cold room using Mini Trans-blot cell (BioRad). In order to prevent excess heating during the run, ice blocks were used and changed after 50 minutes. After the transfer process, the membranes were removed from the cassettes and blocked in 3% BSA on shaker for 1 hour at room temperature. Next, membranes were washed with TBS-T. Primary antibodies to be used were prepared with appropriate dilutions according to manufacturer's instructions in 5% BSA in TBS-T. The membranes were incubated with primary antibody on shaker overnight at 4°C. Each membrane then was washed three times with TBS-T for 5 minutes. After washing, HRP-conjugated anti-rabbit or anti-mouse secondary antibodies were prepared in 5%BSA in TBS-T at 1:5000 dilution. The membranes were incubated in secondary antibody on shaker for 2 hours at room temperature. The membranes then were washed three times in TBS-T for 5 minutes. WesternBright ECL HRP substrate (Advansta) was used for the visualization of proteins according to manufacturer's instructions. Analysis of the blots was performed by using chemiluminescence imaging system (Syngene, UK).

4.2. Total RNA Isolation

Total RNA isolation was carried out with Direct-zol RNA Miniprep Kit (Zymo, USA) according to manufacturer's instructions. Adherent cells on 6-well cell culture plates were washed with 1X PBS. Then, lysis of cells was accomplished in plates by directly adding 300 µl of TRI Reagent onto the cells and mixing thoroughly. Equal volume of 100% ethanol was added to lysed samples in TRI Reagent and the solution was mixed thoroughly. After, the mixture was transferred into a Zymo-Spin IIICG Column in a Collection Tube and centrifuged at 12000g for 30 seconds. The column was transferred into a new collection tube and the flow-through was discarded. 400 µl of Direct-Zol RNA PreWash was added to the column and centrifuged at 12000g for 30 seconds and this step was repeated once more. 700 µl of RNA Wash Buffer was added to the column and centrifuged at 12000g for 2 minutes. The column then was transferred into an Rnase-free tube. Elution was performed by adding 100 µl of Dnase/Rnase-Free Water directly to the column matrix and centrifugation at 12000g for 30 seconds. Total RNA concentration was measured by nanodrop spectrophotometer and $OD_{260/280}$ was checked for any DNA contamination. Isolated RNA samples were used immediately or stored frozen at -80°C until further usage. In order to examine the total RNA integrity, samples were loaded to 1% denaturing agarose gel. The presence of 18S and 28S ribosomal RNAs were confirmed by imaging of the gel.

4.3. Reverse Transcription PCR (RT-PCR)

Total RNA was converted into cDNA by using Promega Reverse Transcription System. 1 µg of total RNA, 1 µl OligodT primers, and nuclease free dH_2O to finalize 5 µl of mix was incubated at 70°C for 5 minutes achieving complete danaturation. Then the reaction mix was immediately cooled down on ice for 5 minutes. The mastermix containing 3.5 µl nuclease free dH_2O, 4 µl 5X reverse transcription reaction buffer, 5 µl $MgCl_2$, 1 µl dNTP, 0.5 µl Recombinant RNasin ribonuclease inhibitor, and 1 µl reverse transcriptase was prepared in an eppendorf tube and distributed into the reaction mixes. The mixture was incubated at RT for 5 min to allow annealing of primers, followed by incubation at 42°C for 1 hour for reaction to occur. As a last

step, reverse transcriptase in the mixture was inactivated at 70°C incubation for 5 minutes. Final products were diluted by 1:5 using nuclease free dH_2O.

4.4. Quantitative Polymerase Chain Reaction

Real Time PCR was carried out with specific primers using Bioline SensiFAST SYBR No-ROX Kit according to the manufacturer's instructions. MGH primer bank encompassing intron/exon junctions was used to choose specific primers for each gene and blasted against target genome for confirmation. The reaction mixtures were prepared and distributed into 96-well qRT-PCR plate, then cDNA templates of each sample were added. The plate was covered with commercially purchased transparent foil and centrifuged at 2000 rpm for 2 minutes. The reaction started with polymerase activation at 95°C incubation for 2 minutes, followed by denaturation at 95°C for 5 seconds, annealing at 61°C for 10 seconds, and finalized with extension at 72°C for 15 seconds. This reaction was repeated for 40 cycles and ended with a melting curve step. Expressions of eaach gene were normalized to GAPDH internal control. Relative expression levels of control and test samples were calculated with the $2^{-\Delta\Delta Ct}$ method which facilitatess semi-quantitative analysis and comparison.

5. RESULTS

The candidate transcriptional targets of the canonical Wnt/β-catenin signaling pathway were previously determined in our laboratory by using two different techniques: genome wide microarray analyses and SAGE (Serial analysis of gene expression). BRI3 was determined to be one of the novel transcriptional targets of the Wnt/β-catenin signaling pathway due to its transcriptional upregulation in HCC cells overexpressing degradation-resistant form of β-catenin and this was further supported with data obtained from lithium treatment of Huh7 cell line, luciferase reporter assay, overexpression of Wnt ligands and chromatin immunoprecipitation (ChIP) assay (Kavak et al., 2010). In order to provide functional relevance of BRI3 with respect to the Wnt/β-catenin signaling pathway, interaction partners were searched by screening a human liver cDNA library. The results showed possible interaction of BRI3 isoform a with MGAT1 and the interaction was further validated by co-immunoprecipitation and colocalization assays. Because MGAT1 was one of the genes that were transcriptionally upregulated in response to ubiquitous activation of the Wnt/β-catenin signaling pathway, this gene was also determined to be one of the novel targets of the Wnt/β-catenin signaling pathway (Akiva, 2018). In this project, contribution of BRI3 and MGAT1 to the development of HCC was investigated in order to explore the molecular mechanisms underlying the process.

5.1. The effect of BRI3 overexpression on selected genes

RNA-Sequencing on tumors derived from Huh7 cells stably expressing GFP or BRI3 in NUDE/SCID mice have indicated several genes that were significantly upregulated or downregulated. Along with pathway enrichment analysis via PANOGA and gene ontology enrichment analysis via Gorilla, candidate genes that were found to be functionally related to carcinogenesis were chosen for further investigation. The resulted genes were YAP1, CSNK2β, and AFP. These genes were selected based on showing the highest fold change values as well as relevance concerning carcinogenesis.

5.1.1. The effect of BRI3 overexpression on mRNA levels of selected genes

In order to investigate the potential role of BRI3 overexpression on hepatocellular carcinogenesis, transient overexpression of BRI3 was provided in Huh7 cells by using constructs prepared previously in our laboratory. RNA samples were collected to compare control and BRI3 overexpressing cells and validate RNA-Seq results obtained before. qRT-PCR was performed by using specific primers for both samples.

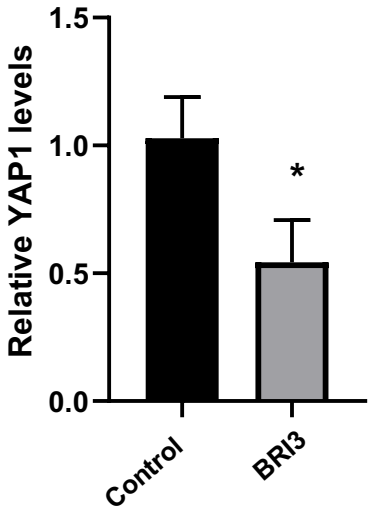

Figure 5.1. The effect of BRI3 overexpression on YAP1 expression levels in Huh7 cells. Columns represent mean + standard deviation. *p<0.05

Figure 5.1 shows the difference in expression levels of YAP1 in control and BRI3 overexpressing groups. As can be seen, YAP1 expression decreased approximately by half in the case of BRI3 overexpression. This result correlates with RNA-Seq results showing Log_2 fold change (Log_2FC) value of YAP1 as -2,034.

CSNK2β expression levels were investigated by performing qRT-PCR experiment by using specific primers amplifying cDNA samples of each group. The expression level of CSNK2β for control and BRI3 overexpressing groups was compared.

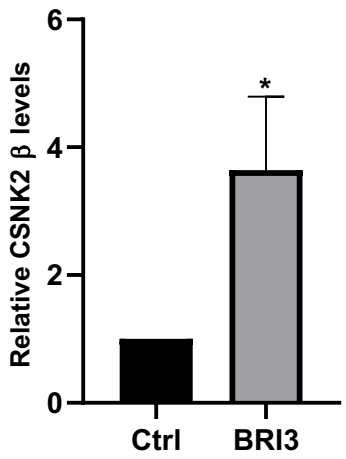

Figure 5.2. The effect of BRI3 overexpression on CSNK2β *e*xpression levels in Huh7 cells. Columns represent mean + standard deviation. *p<0.05

When mRNA levels of CSNK2β for both control and BRI3 overexpressing groups, approximately 3.5-fold change was obtained, as shown in Figure 5.2. The result was compared with the RNA-Seq analysis that that pointed 2,028 Log_2FC and showed correlation.

qRT-PCR experiments were carried out in order to compare and validate the RNA-Seq results that showed 1,928 Log_2FC for AFP expression levels. Specific primers amplifying AFP cDNA samples of both control and BRI3 overexpressing groups were used.

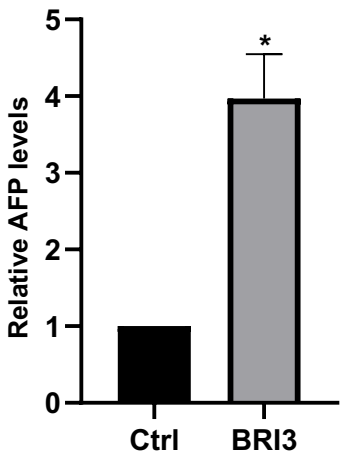

Figure 5.3. The effect of BRI3 overexpression on AFP *e*xpression levels in Huh7 cells. Columns represent mean + standard deviation. *p<0.05

As seen in Figure 5.3, the expression level of AFP in BRI3 overexpressing group have 4-fold increase compared to control. The mRNA levels of AFP in RNA-Seq results had 1,928 Log_2FC.

5.1.2. The effect of BRI3 overexpression on protein levels of selected genes

The second part of the investigations of BRI3 on HCC through Wnt/β-catenin signaling pathway has aimed to reveal the differences in protein levels of selected genes. As a first, YAP1 protein levels have been checked by Western Blot technique. GFP overexpressing samples were used as control.

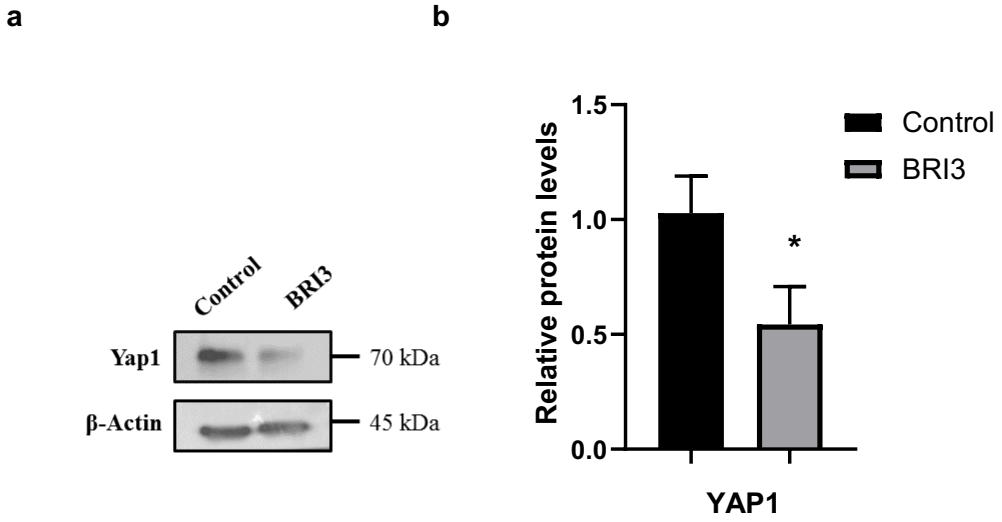

Figure 5.4. The difference in protein levels of YAP1. Protein lysates have been collected from GFP or BRI3 overexpressing Huh7 cells. a) Western Blot results for YAP1. B-actin was used as an internal control. b) Graph of quantitative results of Western Blot. Columns represent mean + standard deviation. *$p<0.05$

In the case of BRI3 overexpression, protein levels of YAP1 have detected to be decreased when compared to control. This decrease was quantified as 2-fold by using ImageJ software. The difference of YAP1 mRNA levels was obtained as -2,034 Log_2FC in the RNA-Seq results previously obtained in our laboratory.

Western Blot experiments have been performed to determine the protein levels of CSNK2β. Control and experimental group were quantitatively compared.

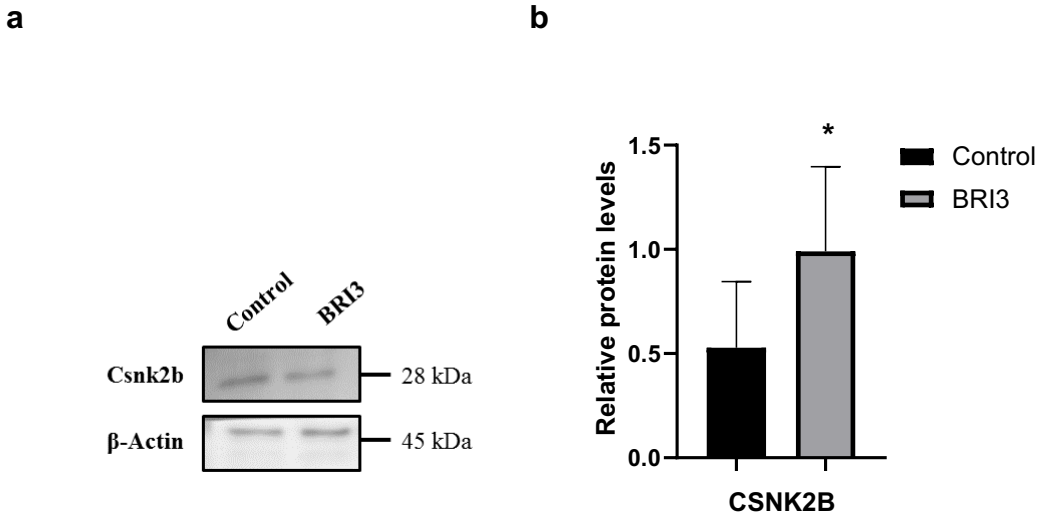

Figure 5.5. The difference in protein levels of CSNK2β. Protein lysates have been collected from GFP or BRI3 overexpressing Huh7 cells. a) Western Blot results for CSNK2β. B-actin was used as an internal control. b) Graph of quantitative results of Western Blot. Columns represent mean + standard deviation. *$p<0.05$

MGAT1 as being a novel target of the Wnt/β-catenin signaling pathway has had an increasing impact on protein levels of CSNK2β kinase in the case of HCC (Figure 5a). This increase has quantified as approximately 2-fold in the protein level similar to mRNA levels (Figure 5b and Figure 2).

The effect of BRI3 overexpression on HCC has been investigated through checking the protein levels of AFP, the gene whose mRNA level had been detected to be increased in the RNA-Seq results.

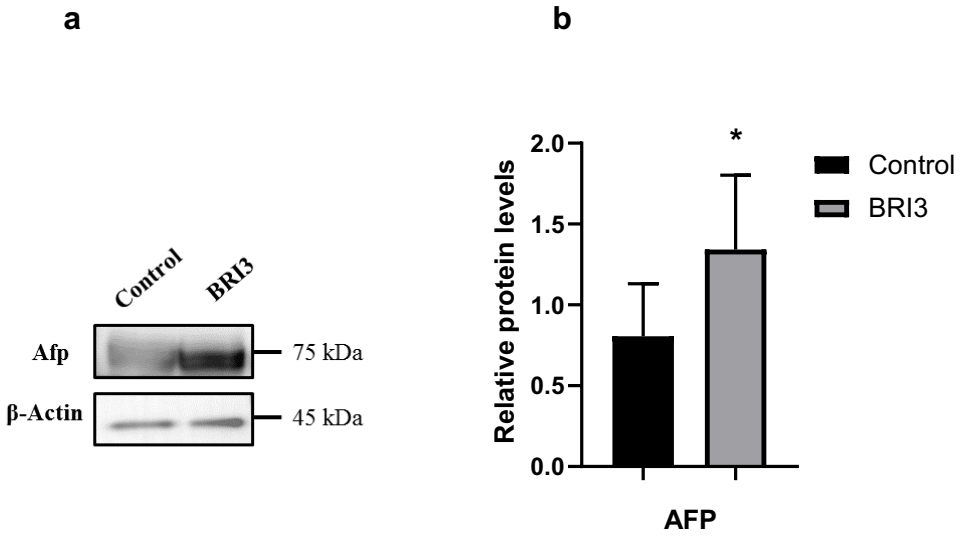

Figure 5.6. The difference in protein levels of AFP. Protein lysates have been collected from GFP or BRI3 overexpressing Huh7 cells. a) Western Blot results for AFP. B-actin was used as an internal control. b) Graph of quantitative results of Western Blot. Columns represent mean + standard deviation. *$p<0.05$

Western Blot experiment results have showed that the BRI3 overexpressing group has almost 2-fold increase in AFP protein levels compared to control group which overexpressed GFP (Figure 5.6b).

5.2. The effect of MGAT1 overexpression on selected genes

RNA-Sequencing of tumors derived from Huh7 cells stably expressing GFP or MGAT1 in NUDE/SCID mice have revealed various genes that were expressed significantly different in control and MGAT overexpressing sample groups. Pathway enrichment analysis via PANOGA and gene ontology enrichment analysis via Gorilla has been applied to RNA-Seq results and three genes were selected to be upregulated or downregulated in the case of MGAT1 overexpression. Overexpression of MGAT1, a novel transcriptional target of Wnt/β-catenin signaling pathway, have resulted in EDNRB, ADAM17, and HSPA8 to be expressed differently in the case of HCC.

5.2.1. The effect of MGAT1 overexpression on mRNA levels of selected genes

The potential role of MGAT1 in hepatocellular carcinogenesis have been investigated by transiently overexpressing MGAT1 in Huh7 cell line. Total RNA samples were collected from both GFP expressing control group as well as MGAT1 overexpressing experimental group. qRT-PCR was performed by using specific primers amplifying EDNRB in each group. Control and MGAT1 overexpressing groups have been compared in order to validate the RNA-Seq results obtained previously in our laboratory.

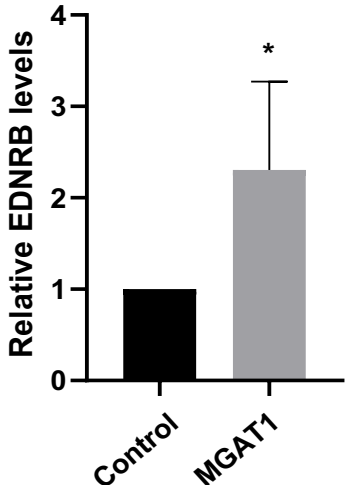

Figure 5.7. The effect of MGAT1 overexpression on EDNRB expression levels in Huh7 cells. Columns represent mean + standard deviation. *p<0.05

MGAT1 overexpression resulted in approximately 2.2-fold increase in EDNRB mRNA levels in Huh7 cell line when compared to control (Figure 5.7). The RNA-Seq results obtained for this gene was found to be 2,332 Log_2FC, validating our qRT-PCR results.

One of the genes that was transcribed significantly different in the case of MGAT1 overexpression was ADAM17 metallopeptidase. When qRT-PCR experiment was carried out, difference in the expression levels of ADAM17 was observed.

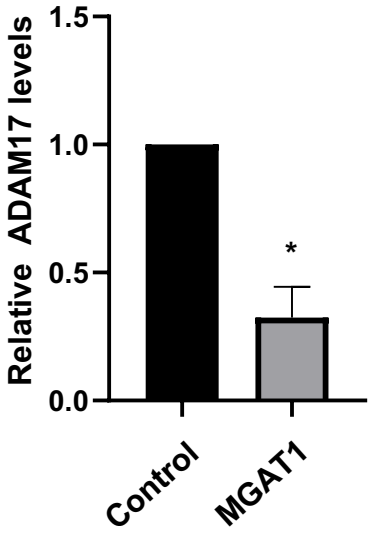

Figure 5.8. The effect of MGAT1 overexpression on ADAM17 expression levels in Huh7 cells. Columns represent mean + standard deviation. *p<0.05

As can be seen in Figure 5.8, qRT-PCR results for ADAM17 showed 3-fold decrease in MGAT1 overexpressing sample group compared to control. RNA-Seq results for ADAM17 was obtained as -2,189, indicating that the difference in the expression level of ADAM17 in MGAT1 overexpressing group was higher since qRT-PCR is considered to be a more precise method than RNA-Seq.

qRT-PCR experiment was also performed with control and MGAT1 overexpressing sample groups in order to compare HSPA8 levels in Huh7 cell line. Previously obtained RNA-Seq results showed downregulation of HSPA8 by 2,287-fold.

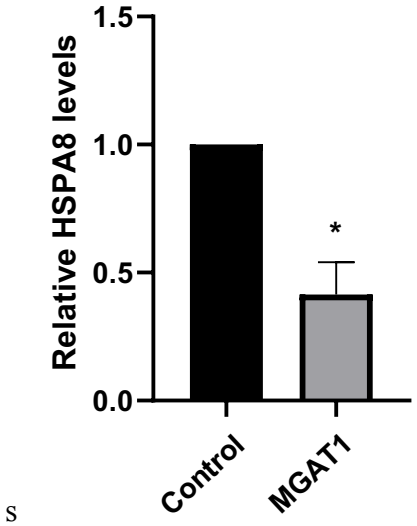

s

Figure 5.9. The effect of MGAT1 overexpression on HSPA8 expression levels in Huh7 cells. Columns represent mean + standard deviation. *p<0.05

The mRNA levels of HSPA8 have decreased by approximately 2.5-fold in MGAT1 overexpressing sample group when compared to control sample group (Figure 5.9). This result correlates with the RNA-Seq results indicating -2,287 Log_2FC for HSPA8.

5.2.2. The effect of MGAT1 overexpression on protein levels of selected genes

Second part of the experiments for investigating the impact of MGAT1 through Wnt/β-catenin signaling pathway on HCC included Western Blot technique in order to determine the protein levels of selected genes. Control group which expressed GFP has been in comparison with MGAT1 expressing sample group.

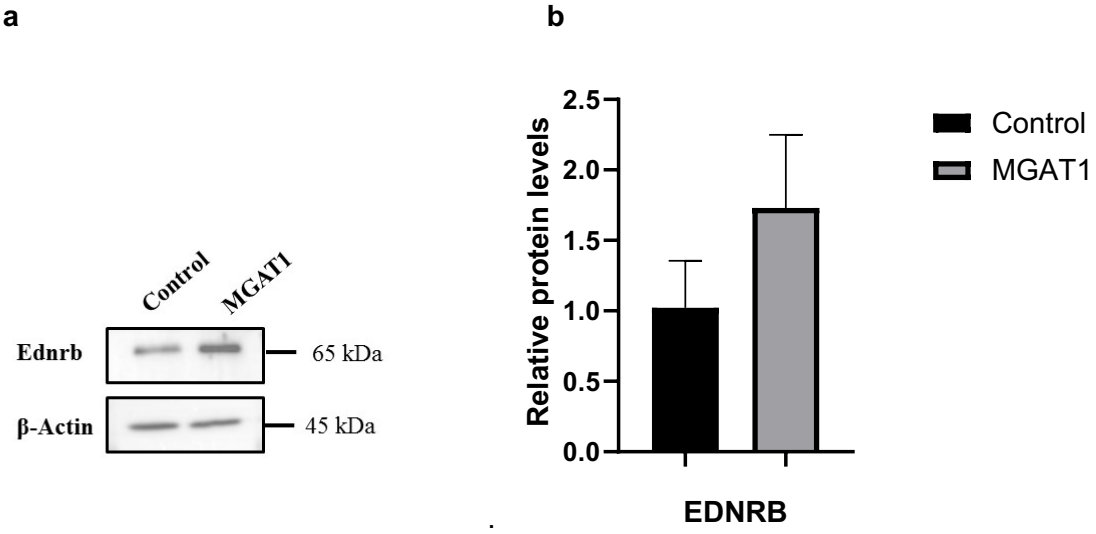

Figure 5.10. The difference in protein levels of EDNRB. Protein lysates have been collected from GFP or MGAT1 overexpressing Huh7 cells. a) Western Blot results for EDNRB. B-actin was used as an internal control. b) Graph of quantitative results of Western Blot. Columns represent mean + standard deviation. *$p<0.05$

Figure 5.10b demonstrates that endothelin type B receptor protein levels have increased by 1.7-fold when MGAT1 was overexpressed. The RNA-Seq results for this receptor had been detected as 2,332 Log_2FC, lower than the increase in the protein level.

ADAM17 metallopeptidase protein levels have also been explored in MGAT1 overexpression conditions. Western Blot results have indicated that protein amount of ADAM17 in MGAT1 overexpressing Huh7 cells had 1.8-fold decrease compared to control (Figure 5.11b). Because RNA-Seq results obtained previously in our laboratory have showed -2,189 Log_2FC, similar change was expected to be seen in the protein level. However, the decrease in the protein level was lower than the decrease in the mRNA level.

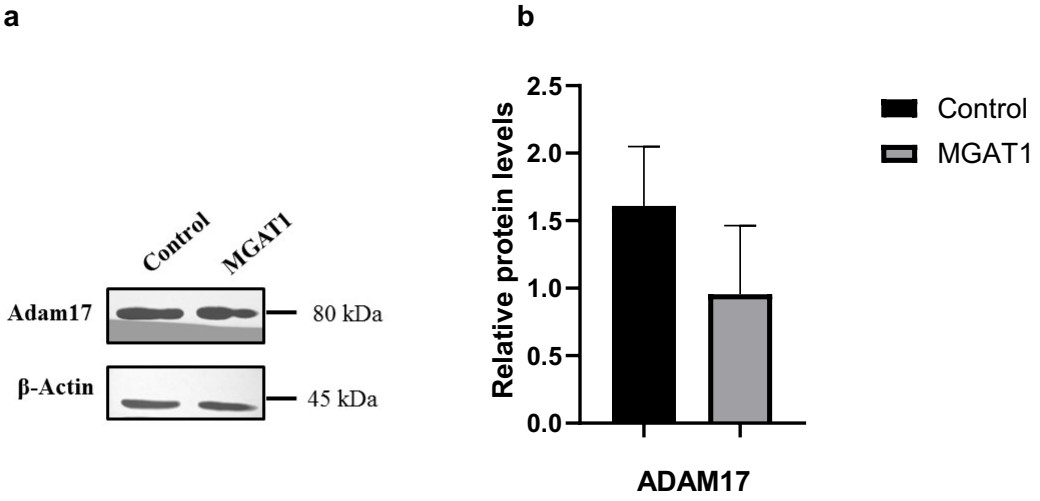

Figure 5.11. The difference in protein levels of ADAM17. Protein lysates have been collected from GFP or MGAT1 overexpressing Huh7 cells. a) Western Blot results for ADAM17. B-actin was used as an internal control. b) Graph of quantitative results of Western Blot. Columns represent mean + standard deviation. *$p<0.05$

Western Blot results have indicated that protein amount of ADAM17 in MGAT1 overexpressing Huh7 cells had 1.8-fold decrease compared to control (Figure 5.11b). Because RNA-Seq results obtained previously in our laboratory have showed -2,189 Log_2FC, similar change was expected to be seen in the protein level. However, the decrease in the protein level was lower than the decrease in the mRNA level.

Western Blot experiments have been performed to determine the protein levels of HSPA8. Control and experimental group were quantitatively compared. In the case of MGAT1 overexpression, protein levels of HSPA8 co-chaperone have detected to be decreased when compared to control. This decrease was quantified as 1.5-fold by using ImageJ software. The difference of HSPA8 mRNA levels was obtained as -2,287 Log_2FC in the RNA-Seq results.

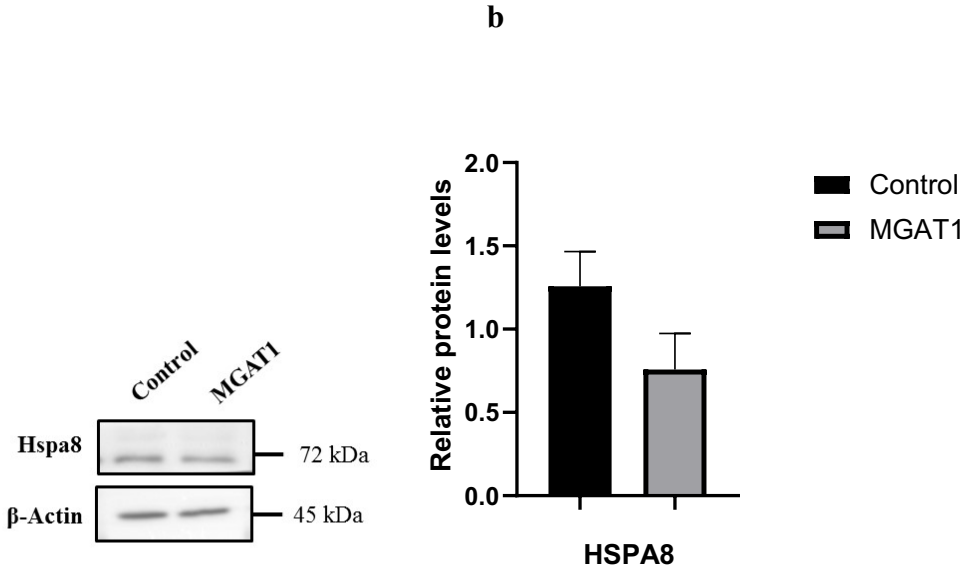

Figure 5.12. The difference in protein levels of HSPA8. Protein lysates have been collected from GFP or MGAT1 overexpressing Huh7 cells. a) Western Blot results for HSPA8. B-actin was used as an internal control. b) Graph of quantitative results of Western Blot. Columns represent mean + standard deviation. *p<0.05

5.3. Bioinformatic Analyses of Protein Interactions

In the last part of the project for BRI3 involvement in HCC, bioinformatic analyses to attempt to reveal the molecular network between candidate proteins has been carried out. As a start, we used the STRING database which operates as a protein-protein interaction network analysis; and for the following, we investigated 3D structures of proteins in PRISM webserver which uses its widespread database of interfaces for protein interactions by structural matching.

5.3.1. STRING Functional Protein Association Network Analysis

STRING is a global database of both known and predicted protein-protein interactions, including both physical and functional associations. It uses a computational prediction from

knowledge of different organisms as well as interactions collected from other databases (Szklarczyk *et al.*, 2018).

Selected genes based on their significant difference in expression levels as a result of RNA-Seq analysis by using samples taken from tumors derived from Huh7 cells stably expressing either GFP as control or BRI3 as the experimental group were investigated for physical or functional interactions. STRING database was used to determine if there were such interactions between YAP1, CSNK2β, and AFP along with BRI3. Several more proteins which are found in pathways of YAP1, CSNK2β, and AFP as well as some other proteins known to be related to these pathways were added to the input in STRING database server.

Since there are no previous studies in the literature that positions BRI3 in any known pathway or functionally relates it to any of our proteins of interest, BRI3 was not found to interact physically or functionally, as expected. However, although no relations between YAP1, CSNK2β, and AFP have been demonstrated in the literature, YAP1 was shown to physically interact with CTNNB1 gene, a gene that synthesizes the key protein β-catenin of Wnt/β-catenin signaling pathway. In addition to YAP1, CSNK2β was also found to interact with β-catenin.

EDNRB, ADAM17, and HSPA8 genes that were proved to be either upregulated or downregulated in the case of MGAT1 overexpression were investigated for physical or functional interactions. Several more proteins that are found to be in relation to EDNRB, ADAM17, and HSPA8 as well as some other proteins known to be related to pathways these proteins participate in were added to the input in STRING database server.

Figure 5.14 demonstrates that there are no physical or functional interactions between MGAT1 and EDNRB, ADAM17, and HSPA8 proved previously in the literature. Nonetheless, it can be asserted that these proteins may have interactions through signaling pathways. When STRING database results were examined, several different interactions have been observed.

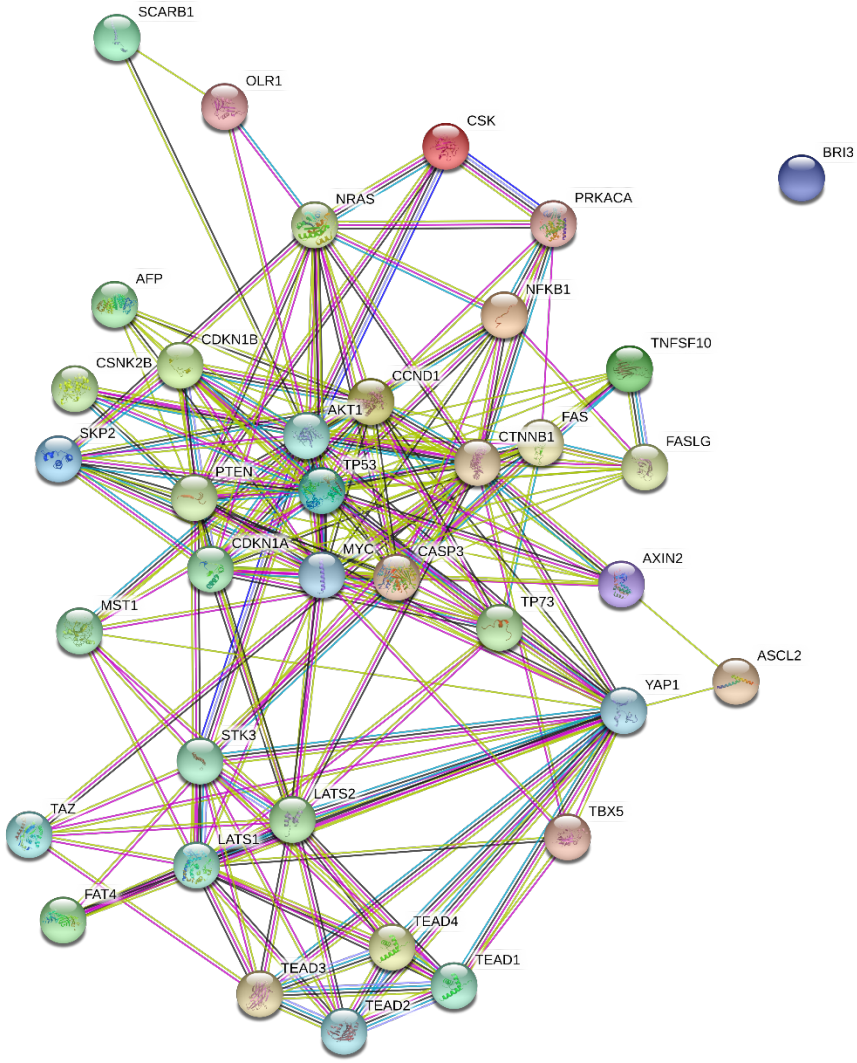

Figure 5.13. Physical and functional protein-protein interaction analysis for BRI3 and its predicted downstream proteins by using STRING database.

As a first, a study shows CD9 tetraspanins and catalytically active form of ADAM17 colocalize on the surface of keratinocytes in the course of wound repair *in vivo* and *in vitro*. Additionally, inhibition of the sheddase activity of ADAM17 decreased the release of HB-EGF shedding in CD9-silenced HaCat cells and C57MKs (Liu *et al.*., 2019). In another study, CD9 tetraspanin expression was shown to induce the exosomal release of β-catenin and strongly

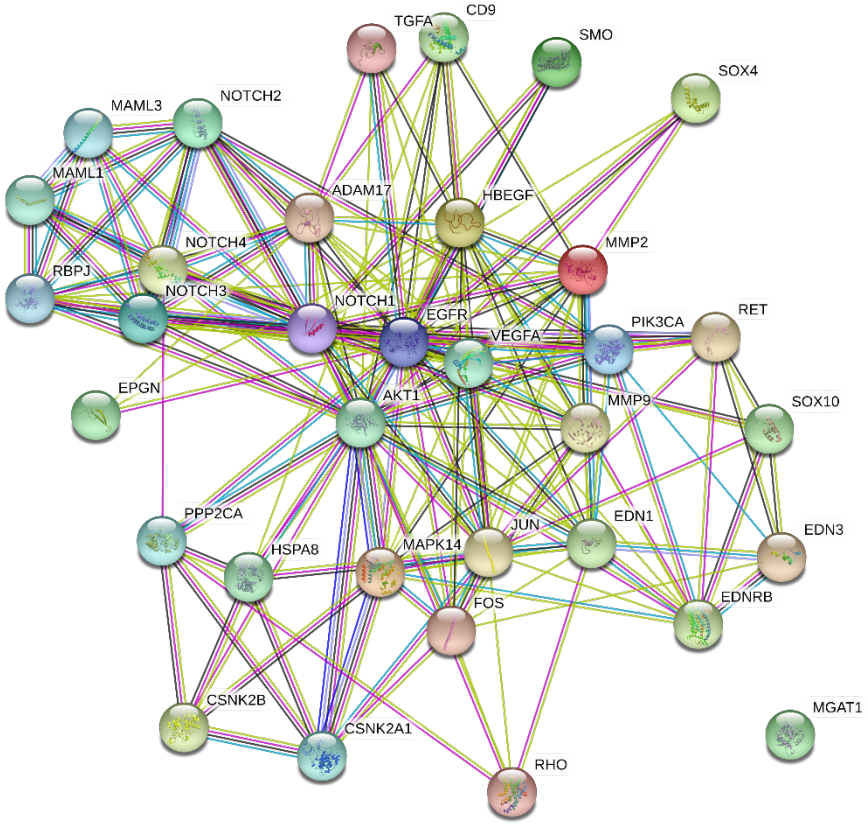

Figure 5.14. Physical and functional protein-protein interaction analysis for MGAT1 and its predicted downstream proteins by using STRING database.

supresses β-catenin-mediated Wnt signaling activity (Chairoungdua *et al.*, 2010). Giving the fact that cells expressing ADAM17 in high levels would have small amounts of CD9, the secretion of β-catenin via exosomes is expected to be less. This decrease in the exosomal release also results in less secretion of HSPA8 co-chaperone via exosomes (Hessvik & Llorente, 2018).

STRING protein-protein interaction analysis for MGAT1 and its downstream selected genes have revealed an indirect interaction between ADAM17 and EDNRB (Figure 5.14). Sahin and his colleagues introduced ADAM17 as the major convertase of HB-EGF in mouse embryonic cells (Sahin *et al.*, 2004). Furthermore, a study from 2017 demonstrated several outcomes by GO analysis of differentially expressed genes such as most enrichment for genes associated with regulation of cell proliferation, including HB-EGF which was upregulated by

Wnt3a, and enrichment for genes associated with cell migration, including EDNRB which was downregulated by Wnt3a (Sebastian *et al.*, 2017). On the contrary, our study validated that ADAM17 was downregulated, and EDNRB was upregulated in the case of MGAT1 overexpression.

Another indirect interaction was observed between HSPA8 co-chaperone and endothelin type B receptor. DNA binding activity of AP-1, a variable complex of Fos and Jun family proteins has shown to be attenuated by Hsps including HSPA8 through a mechanism that influences the assembly of protein complexes (Carter, 1997). Besides, endothelin type B receptor-ligand ET-1 was found to inhibit c-Jun synthesis via EDNRB and thus has an anti-proliferative effect on hepatic stellate cells (HSC) (B *et al.*, 1996).

5.3.2. PRISM Protein Interactions by Structural Matching

An online tool termed PRISM (protein interactions by structural matching) developed by Koç University team Baspinar and his colleagues provides a protocol for prediction of protein-protein interactions and assembly of protein complex structures (Baspinar *et al*., 2014)(Tuncbag *et al*., 2011). The method contains comparisons of rigid-body structures of target proteins to known template protein-protein interfaces along with flexible refinement using a docking energy function. It depends on the fact that globally different protein structures interact via similar architectural motifs, and predicts binding residues benefiting from structural similarity and evolutionary conservation of putative binding residue 'hot spots'. PRISM repository stores predicted models. Data Bank-formatted protein structures are accepted in the program that is implemented in python, runs in a unIX environment and is available at http://prism.ccbb. ku.edu.tr/prism_protocol/.

In the last part of the project, we carried out structural matching analysis by using crystal structures of selected proteins and BRI3. Unfortunately, there is no crystal structure studies on BRI3 protein in the literature so we could not include BRI3 in our search for protein-protein interactions. Crystal structures to use in PRISM online tool was obtained from RCSB protein

data bank archive. Protein interactions analysis resulted in a potential interaction between CSNK2 tetrameric holoenzyme and YAP1 protein in complex with TEAD transcription factor (Figure 5.15).

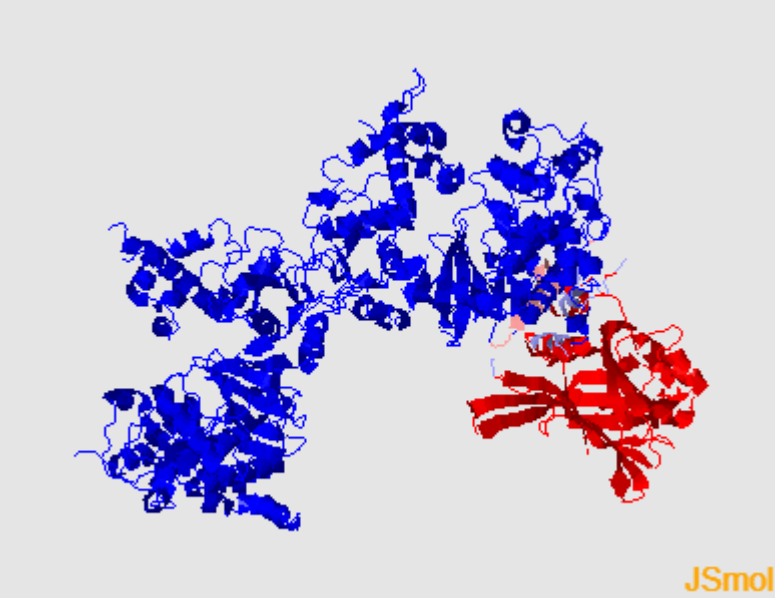

Figure 5.15. PRISM results of YAP1 protein in complex with TEAD transcription factor (blue) and CSNK2 tetrameric holoenzyme (red). The interface is shown in pink.

Figure 5.15 demonstrates the interface of direct interaction between YAP1 protein in complex with TEAD and CSNK2 tetrameric holoenzyme. The energy score of this interaction was calculated as -2.83. Some residues significant at the interface (coded as 2hqtAC in PRISM server) were G90 - M73, P92 - L6, and H168 - G310.

PRISM online tool for interaction analysis by structural matching was used for MGAT1 and selected genes. Several interactions between proteins was found. MGAT1 crystal structure obtained from X-Ray diffraction showed interaction with the ligand-bound form of EDNRB (Figure 5.16). The energy score was calculated as -62.51 for the interface coded as 3dzcAB in the database of the server. Several important residues at the interface were L145 - P205, I153 - V107, and S120 - N203. We found another interface named 1zp4AC with -53.92 energy score

for the interaction between two transmembrane proteins. The interface included interacting residues M173 - N201, M173 - N203, Y127- W299, and V223-P235. The crystal structure of MGAT1 also showed interaction with the ligand-free form of EDNRB with energy scores of -55.62 (Figure 5.17), -51.32, -50.3, and 45.7. The interactions were observed from the transmembrane region of EDNRB therefore is not possible *in vivo*.

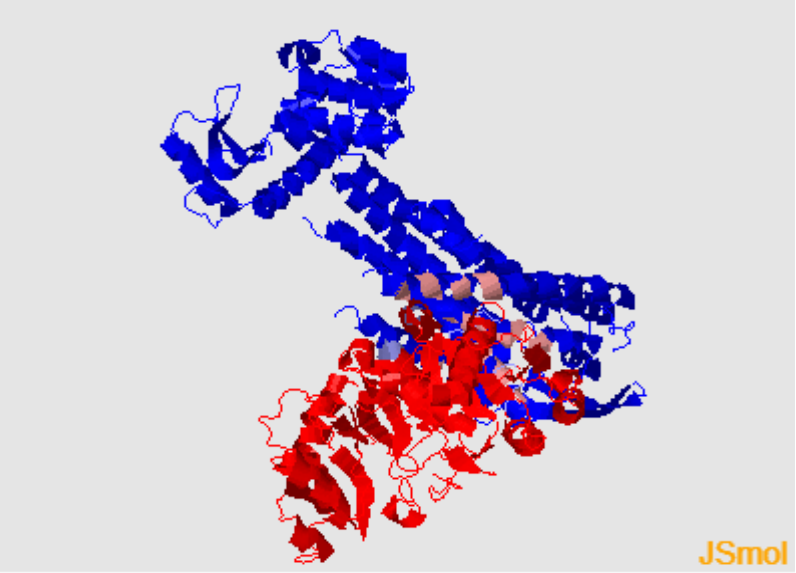

Figure 5.16. PRISM results of MGAT1 protein (red) and EDNRB protein with its ligand ET-1 (blue). The interface is shown in pink.

PRISM interaction analysis by structural matching revealed another direct interaction between MGAT1 enzyme and ADAM17 metallopeptidase, with energy score of -22.18 (Figure 5.18). This interaction was detected as MGAT1 interacting with EDNRB hydrophobic transmembrane region therefore is not possible *in vivo*.

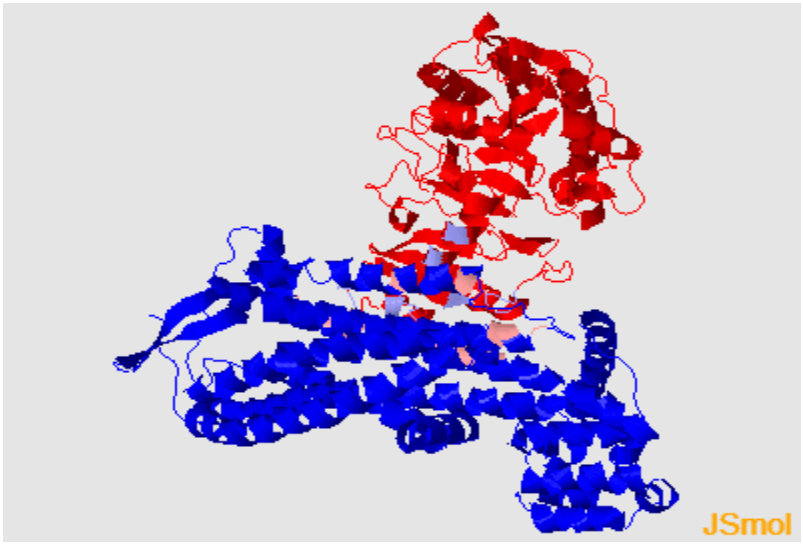

Figure 5.17. PRISM results of MGAT1 (red) and the ligand-free form of EDNRB (blue) proteins. The interface is shown in pink.

The interface of the direct interaction between MGAT1 and ADAM17, coded as 1gyIAB, included several important residues such as D416 - R358, E468 - P368, and S457 - A362. 2vscAB interface was also found between MGAT1 and ADAM17 with the energy score of -4.44. MGAT1 in complex with UDP-glucose also showed interaction with the catalytic domain of ADAM17 (Figure 5.19).

The energy score of MGAT1 in complex with UDP-glucose and the catalytic domain of ADAM17 was calculated as -6.1 with the interface of 3sf8AB in the PRISM webserver. Some significant residues of the interaction can be given as R257 – H147, T246 – S156, N249 – E148, and T246 – V153.

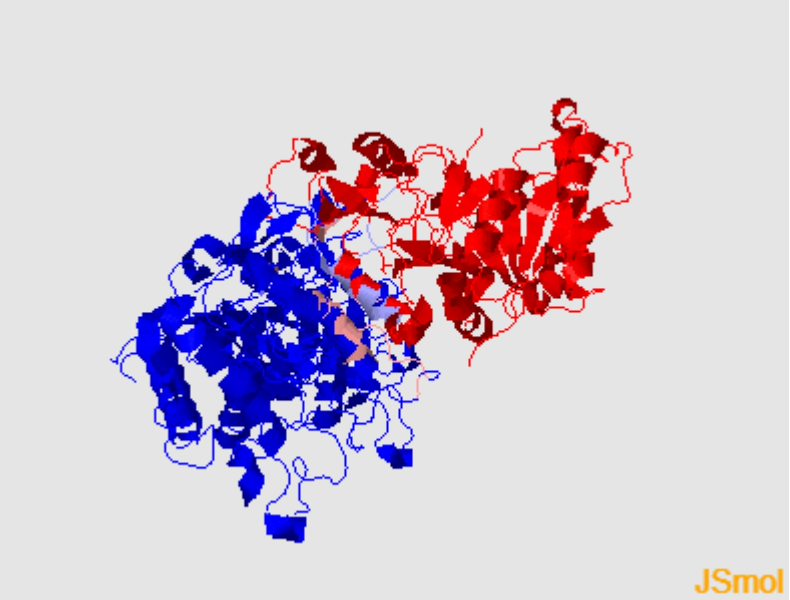

Figure 5.18. PRISM results of MGAT1 (blue) and ADAM17 (red) proteins. The interface is shown in pink.

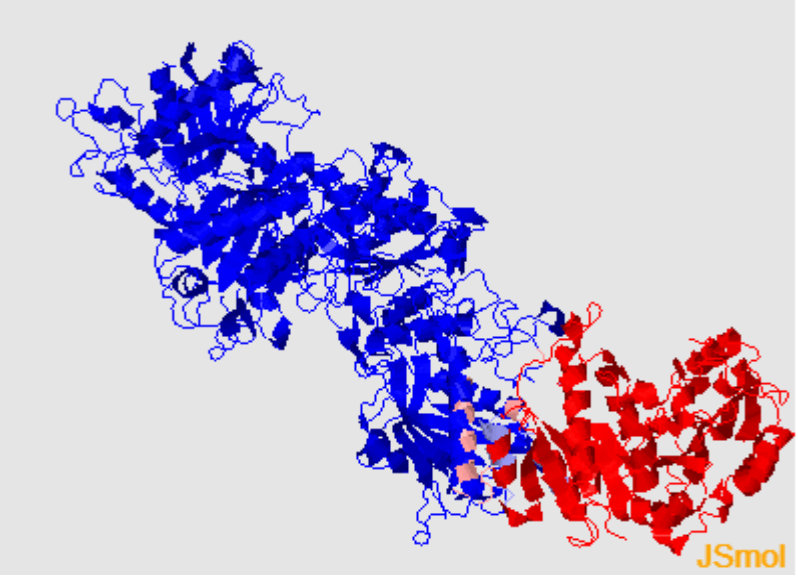

Figure 5.19. PRISM results of MGAT1 in complex with UDP-glucose (blue) and the catalytic domain of ADAM17 (red) proteins. The interface is shown in pink.

Finally, another direct interaction between MGAT1 and HSPA8 in complex with BAG1 co-chaperone was found (Figure 5.20). The interface was determined as 3t5pAH in the PRISM webserver, and the energy score was calculated as -16.46. Examples of important residues at the contact site are D152 – Q152, N168 – R165, N168 – Q166, and T140 – P167. In addition, one more interface for this interaction was detected with a lesser energy score, being -4.64. This interface between MGAT1 and HSPA8 in complex with BAG1 co-chaperone was named as 2fw7AB.

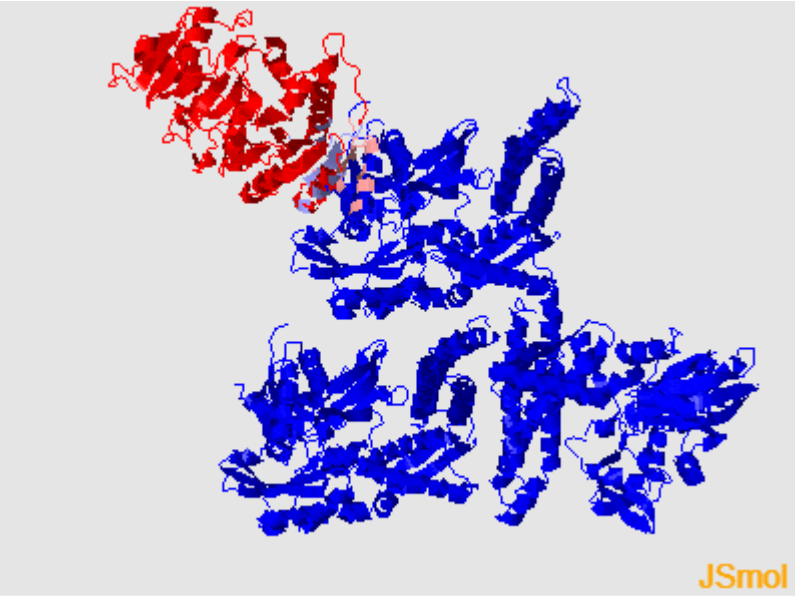

Figure 5.20. PRISM results of MGAT1 (red) and HSPA8 in complex with BAG1 (blue) proteins. The interface is shown in pink.

6. DISCUSSION

The canonical Wnt/β-catenin signaling pathway is an evolutionarily conserved pathway and controls several mechanisms such as embryonic development and adult homeostasis. The key protein, β-catenin, is translocated into the nucleus when a signal through secreted glycoproteins of the Wnt family activates the Wnt/β-catenin signaling pathway. β-catenin is a transcriptional activator which operates as a regulator of gene expression programs affecting cellular proliferation, differentiation, and morphogenesis. Wnt/β-catenin signaling pathway, when aberrantly activated, has the potential to initiate tumorigenesis; hence, the pathway and its targets are important subjects in the cancer research fields. Genes that are regulated by this pathway are potential drug and gene therapy targets thus it is crucial to reveal the full mechanism and identify novel transcriptional targets.

Our laboratory began to study Wnt/β-catenin signaling pathway to find novel transcriptional targets via SAGE and microarray screens. By providing the active status of the Wnt/β-catenin signaling pathway in several ways, some genes were detected to be significantly upregulated or downregulated. Using overexpression strategy of the degradation-resistant β-catenin mutant (S33Y- β-catenin), and providing supporting data from lithium treatment of Huh7 cells, luciferase reporter assay, and ChIP; BRI3 was determined to be one of the novel targets of Wnt/ β-catenin signaling pathway (Kavak *et al.*, 2010).

Continuing studies of the Wnt/β-catenin signaling pathway, MGAT1 was also identified as a novel transcriptional target since it was determined to be an interacting partner of BRI3, was one of the genes which exhibited differential expression in response to activation of the pathway, and also was included among the candidate target genes with respect to the SAGE analysis (Akiva & Birgül Iyison, 2018). BRI3 and MGAT1 were found to colocalize inside an organelle, possibly in the Golgi apparatus or ER.

Our laboratory aimed to characterize the novel targets of the Wnt/β-catenin pathway via several methods. Cell proliferation and migration assays demonstrated that, Huh7 cell lines stably overexpressing either BRI3 or MGAT1 have greater proliferative and invasive capabilities when compared to control Huh7 cells. Besides, *in vivo* xenograft experiments showed that when subcutaneously injected into NUDE/SCID mice, Huh7 cells stably overexpressing of either of these genes result in larger tumor formation. These findings led our colleagues to use RNA-Sequencing technique in samples taken from control tumors or tumors overexpressing BRI3 or MGAT1 to demonstrate the pathways and biological processes that might contribute to hepatocellular cancer.

RNA-Seq analysis revealed several genes that are differentially expressed in the case of BRI3 or MGAT1 overexpression in tumors. By using this technique, determination of transcript levels at a given time and condition is accomplished. Upregulated and downregulated genes in either BRI3 or MGAT1 overexpressing tumors were ascertained separately. Among the genes, a few potential targets of the Wnt/β-catenin pathway which have important roles in tumor formation were able to be specified. In BRI3 overexpressing tumors, YAP1, CSNK2β, and AFP genes were found to be expressed significantly different as compared to control. In this study, we aimed to verify the differential expression levels of the selected genes via qRT-PCR technique and investigate the protein levels of these genes via Western Blot technique. Furthermore, we attempted to unravel the mechanism of interactions between these genes in the context of HCC by using bioinformatic tools.

Transcriptomic analysis of BRI3 showed -2.034 Log_2FC for YAP1 in BRI3 overexpressing samples when compared to control. This change was verified by qRT-PCR experiments as we obtained approximately a half reduction in YAP1 mRNA levels in BRI3 overexpressing Huh7 cells (Figure 5.1). In this way, the expected results were achieved and the precision quality of the RNA-Seq results was clarified as they demonstrated the same results with the qRT-PCR results. Western Blot analysis indicated similar levels of change between GFP-overexpressing control Huh7 cells and BRI3-overexpressing Huh7 cells (Figure 5.4b). The experiments were repeated at least five times and the results were obtained as significantly

different ($p<0.05$). Taken together, these results point out that the regulation of this gene controlled by BRI3 should be at the transcriptional level or RNA processing level because the protein levels of YAP1 did not differ from the mRNA levels. The contribution of YAP1 to HCC through BRI3 might also be relevant to the protein activity control of YAP1 which occurs largely through covalent post-translational modifications including phosphorylation, ubiquitylation, and acetylation.

YAP1, Yes-associated protein, is a downstream nuclear effector of the Hippo signaling pathway which is associated with development, growth, repair, and organ homeostasis. As a transcriptional regulator of the Hippo pathway, YAP1 plays a decisive role in the development of primary liver cancer and is frequently amplified in various types of cancer including liver, prostate, breast, and esophageal cancer (Harvey & Tapon, 2007). YAP1 upregulation in liver cancer is reported in the currently available data; in fact, increased YAP1 activity is a driving event for liver cancer (Nguyen, Anders, Alpini, & Bai, 2015). There are also several studies indicating the upregulation of YAP1 mRNA and protein levels in the context of HCC, and this upregulation was frequently associated with reduced survival rate in patients (Harvey, Zhang, & Thomas, 2013; Shi *et al*., 2018). Hippo pathway transducers YAP/TAZ have been shown to play mixed roles in Wnt signaling but the underlying mechanism is yet to be discovered. YAP/TAZ complex was shown to be a part of the β-catenin destruction complex and the upregulation of YAP resulted in β-catenin degradation. The same study also demonstrated that, when Wnt is on, YAP/TAZ complex is released from the destruction complex and translocated in the nucleus to activate the transcription of YAP/TAZ/TEAD target genes (Azzolin *et al.*, 2014). Considering YAP1 expression levels, in a more recent study, researchers demonstrated high expression levels for YAP1 in the mixed type of liver cancer, hepatocellular–cholangiocarcinoma (cHCC-CCA) but low expression in HCC (Van Haele *et al.*, 2019). In this study, we validated that, in the case of BRI3 overexpression, a novel target of the Wnt/β-catenin signaling pathway, YAP1 mRNA and protein levels decreased by half in Huh7 hepatocellular cell lines. YAP1 functions as a tumor suppressor in HCC cell lines, coinciding with another study indicating YAP1 as a tumor suppressor in breast cancer (Yuan *et al*., 2008). Our results may be interpreted as this effect exclusive of BRI3 upregulation on YAP1 expression levels in

HCC since YAP1 plays various roles in different contexts of cancer. YAP1 might have both oncogenic and tumor suppressive functions in a context-dependent manner as previously reported for other factors in different types of cancer (Rowland & Peeper, 2006).We also investigated the expression levels of other components of the Hippo pathway and realized that when BRI3 is upregulated, TAZ and LATS1 are too downregulated as YAP1 but not MST1 (data not shown). Therefore, we propose that BRI3 upregulation as a result of Wnt pathway activation leads to Hippo pathway inactivation by being affected from the LATS1 level since LATS1, the inhibitor of YAP/TAZ complex is downregulated. Contrary to expected, YAP/TAZ levels are also downregulated in BRI3 overexpressing cells, but we do not have the knowledge of whether YAP1 is phosphorylated and in its inactive form or not. Also, as mentioned above, YAP1 might function as a tumor suppressor in the context of HCC. Consequently, because LATS1 levels decreased in BRI3 overexpressing cells, YAP1 phosphorylation should be lesser than control group, which may be interpreted as inactivation of the Hippo pathway and subsequently enhanced cell proliferation and tumor growth. However, downregulation of YAP1 in Huh7 cells might rely on some other mechanism rather than the core Hippo cascade regulating YAP1 expression.

CSNK2β gene was also studied due to its upregulation in the case of BRI3 overexpression in Huh7 cells. This upregulation was obtained as 2,028 Log_2FC in the RNA-Seq analysis. However, the upregulation of CSNK2β mRNA levels in samples taken from BRI3 overexpressing cells was calculated as 3.5-fold in qRT-PCR experiments (Figure 5.2). The experiments were repeated several times and the result was realized significantly changed ($*p<0.05$). Additionally, the protein levels of CSNK2β were also investigated and measured as 2-fold increase in BRI3 overexpressing group compared to control (Figure 5.5). These observations led us to think that the half-life of the protein might be substantially short *in vivo*, or that some specific miRNAs targeting CSNK2β induces downregulation of the mRNA. Moreover, post-transcriptional modifications of the mRNA (RNA processing) which determine the faith of the mRNA in cells could also be responsible for low protein levels.

CSNK2β, casein kinase 2β, is the beta subunit of a tetrameric holoenzyme CK2, a ubiquitous serine/threonine protein kinase which regulates metabolic pathways, signal transduction, replication, transcription, and translation. The beta subunit of CK2 serves regulatory functions. The enzyme localizes to the cytoplasm, nuclei, Golgi apparatus as well as the endoplasmic reticulum. CK2 has a key regulatory role in cell proliferation, differentiation, and apoptosis; and participates in Wnt signaling. Song *et al.* showed that CK2 inhibition decreases the level of β-catenin and halts proliferation of Wnt transfected cells, suggesting that β-catenin phosphorylated by CK2 avoids ubiquitination and subsequent degradation (Song, Sussman, & Seldin, 2000). Another group of researchers indicated that the activity of CSNK2β is increased rapidly and transiently in response to Wnt3a stimulation and is essential for Wnt/β-catenin signaling (Gao & Wang, 2006). This transient increase of CSNK2β activity gives us a clue about the regulation of CSNK2β protein expression reduced post-transcriptionally by the Wnt pathway. CK2 acts as a positive regulator of the Wnt signaling (Seldin *et al.*, 2005). When CSNK2β is considered within the context of HCC and as its upregulation was due to overexpression of BRI3, we may say that the kinase could be involved in the positive feedback loop of the Wnt signaling pathway via BRI3. We hypothesize that the upregulation of BRI3, downstream target of the Wnt pathway, resulted in the upregulation of CSNK2β in Huh7 cells, hence further activation of the Wnt pathway.

Previous study in our laboratory demonstrated that BRI3 might form a complex with TRAF2 and TRAF6, adapter proteins in the signal transduction of NFkB pathway (Akiva, 2016). NFkB pathway activation is a frequently seen early event in human liver cancers and is associated with cancer progression in HCC (Luedde & Schwabe, 2011). There are strong associative and functional links suggesting that CK2 act on both NFkB and Wnt signaling to promote tumorigenesis in the mammary gland (Dominguez, Sonenshein, & Seldin, 2009). CK2 acts at multiple levels in the activation of NF-kB pathway, as it targets not only the inhibitor IkB (Romieu-Mourez, 2001), but also IKK-i/IKKε upstream (Eddy *et al.*, 2005), and NFkB p65 itself (Chantôme *et al*., 2004)(Wang, *et al.*, 2000). We have also mentioned above that CK2 acts as a positive regulator of the Wnt pathway. Considering the knowledge in literature, we propose

that CK2 is functionally linked to both Wnt and NF-kB pathway via the mediator BRI3 and play a central role in hepatocellular carcinogenesis.

Our findings from PRISM webserver analysis indicate that YAP1 in complex with TEAD transcription factor physically interacts with CK2 tetrameric holoenzyme (Figure 5.15). It is at our knowledge that CK2 is a pleiotropic enzyme which has over 300 known substrates so far (Pinna, 2002). However, the energy score of the interaction (-2.83) is not enough for YAP1 to be a substrate of CK2. In order to evaluate the strength and the stability of the interaction proposed by PRISM, molecular dynamics simulation (at least 50 ns) should be run.

Next, we aimed to investigate the mechanism of AFP involvement controlled by the Wnt pathway in HCC. As a novel target of the Wnt pathway, we overexpressed BRI3 and compared the expression levels of AFP between control and BRI3 overexpressing Huh7 cells. AFP mRNA levels increased 4-fold (Figure 5.3) and the protein levels increased 2-fold in BRI3 overexpressing Huh cells (Figure 5.6). qRT-PCR results indicate that the precise quantification of AFP mRNA level increase in BRI3 overexpressing cells was higher than 1.928 Log_2FC value obtained from RNA-Seq analysis. Also, the increase in protein level of AFP was lower than the mRNA level, indicating similar regulations that of CSNK2β might contribute to the expression levels of AFP in Huh7 cells. In fact, AFP mRNA is shown to be a direct substrate for the nuclease activity of Regulated Inositol-Requiring Enzyme-1α (IRE-1α), one of the arms of unfolded protein response in HCC cells (Houessinon *et al.*, 2016).

AFP, alpha-fetoprotein, is a glycoprotein expressed mostly in liver and yolk sac during fetal development but is gradually repressed by the age of 8 to 12 months (Breous & Thimme, 2011). However, high expression levels of AFP are detected in the blood of most HCC patients and it is therefore used as a marker of the aggressiveness of the tumor (Buendia & Neuveut, 2019; Gao et al., 2016). AFP protein is thought to be the fetal counterpart of serum albumin, and the albumin and AFP genes are present in tandem on chromosome 4.

AFP is involved in pleiotropic activities, influencing important processes like cell differentiation, regulation of growth, and tumorigenesis (Muehlemann *et al.*, 2005). Li and his colleagues demonstrated that the presence of AFP virtually abolished the caspase-3 pathway involved in TRAIL-induced apoptosis in Bel 7402 HCC cell line (Li *et al.*, 2007). There is a possibility that higher levels of AFP in BRI3-overexpessing cells correlates with the escape of HCC cells from apoptosis. Overexpression of AFP promoted the activation of canonical Wnt signaling and increased the transcription of target gene c-MYC to enhance growth and metastasis in AFP-producing gastric cancer (APCC). Furthermore, Wnt pathway blockade by overexpression of Axin1 or small-molecule inhibitor XAV939 disrupted AFP-mediated malignancy in APGC (Chen *et al.*, 2019). Our study presents AFP as downstream of the Wnt pathway and its target gene BRI3, but it may have a dual role as it is also responsible for the activation of the Wnt pathway in APGC. AFP upregulation by BRI3 overexpression might increase c-MYC signaling pathway activity thus enhance growth and metastasis in HCC. The role of AFP on different cell signaling pathways is crucial in HCC aggressiveness and survival rate; and the mechanism could be through binding to nuclear receptors including all *trans*-retinoic acid (ATRA) receptors and acting as a transcription-associated regulatory factor as previously demonstrated (Dauphinée & Mizejewski, 2002). Further investigations on the function of AFP will shed light on the mechanism of AFP action in HCC.

As another novel target of the Wnt signaling pathway determined by our laboratory, we investigated the possible role of MGAT1 gene in hepatocellular carcinogenesis. For this purpose, we overexpressed MGAT1 gene in Huh7 cells and compared the difference on expression levels of three genes that were previously selected based on their differential expression in the transcriptomic analyses. EDNRB was one of the genes that were detected to be upregulated by 2.33-fold in MGAT1 overexpressing tumors compared to GFP expressing tumors in RNA-Seq results. qRT-PCR experiments indicated the difference between control and MGAT1 overexpressing groups as 2.2-fold increase in the latter (Fig 5.7). Protein levels of EDNRB were also checked and obtained as 1.7-fold in MGAT1 overexpressing Huh7 cells (Figure 5.10).

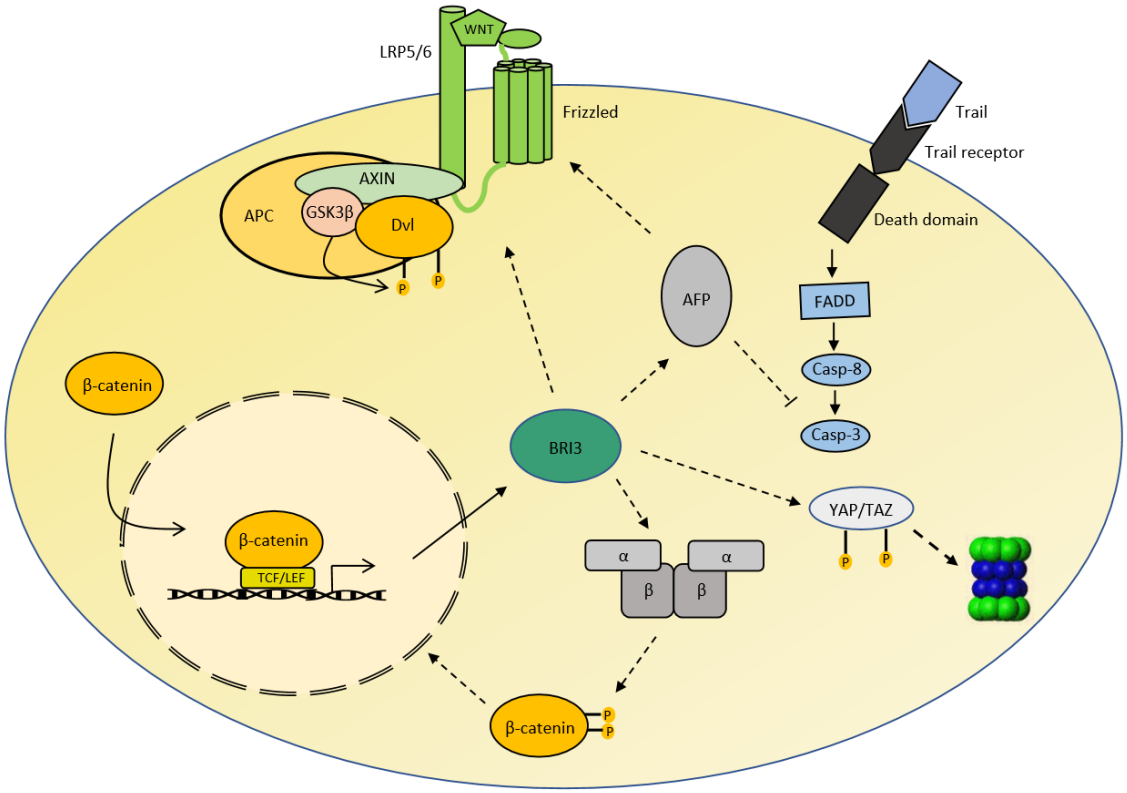

Figure 6.1. Schematic representation of the hypothesized mechanism of BRI3 contribution to HCC.

Endothelin receptor type B is a rhodopsin-like G protein-coupled receptor activating a phosphatidylinositol-calcium second messenger system. It is one of the two (type A and type B) non-specific receptors for a family of three potent vasoactive peptides E1, E2, and E3. ET_B normally promotes apoptosis and clearance of ET-1 in cells (Bremnes *et al.*, 2000).

The ET axis has an important role in various cancer cells which promotes tumorigenesis via autocrine/paracrine feedback loops such as cell proliferation, escape from apoptosis, metastasis, and angiogenesis (Nelson *et al.*, 2003). Activation of ET_B was observed in different types of cancer. Overexpression of ET_B was shown in melanomas (Lahav, 2005) and oligodendrogliomas (Anguelova *et al.*, 2005); and correlated with malignant melanoma development and progression (Lahav, 2005). In addition, immunohistochemical analysis and

gene expression profiling of human melanoma cell lines and biopsies indicated ET_B as an agressive phenotype associated tumor progression marker (Demunter *et al.*, 2001). ET1 has been found to directly promote tumor angiogenesis by inducing endothelial cell survival, proliferation, and invasion via binding to ET_B, also indirectly by upregulating VEGF production in the vasculature and through activating ET_B (Jesmin *et al.* , 2006; Salani *et al.*, 2000). Also, strong correlation between ET_B and VEGF expression in diferent tumor specimes have been observed (Kato *et al.*, 2001). PRISM proposed a possible physical interaction between MGAT1 and ET_B (Figure 5.17) with a strong energy score -55.62; however, the interaction was observed through the transmembrane region of ET_B and is impossible to occur *in vivo*. Previous and current data combined, we can hypothesize that aberrant activation of Wnt pathway leads to upregulation of MGAT1, and in turn, MGAT1 regulates the upregulation of ET_B in an unknown mechanism. MGAT1 overexpression was shown to cause more proliferative and invasive tumors in mice, and it might be through increased tumor angiogenesis and upregulating VEGF via ET_B.

The next gene to be chosen that was differentially expressed in MGAT1 overexpression in tumor samples was ADAM17 with Log_2FC of -.2.189. The mRNA levels of ADAM17 in MGAT1 overexpressing Huh7 cells were 3-fold lower than control (Figure 5.8) and the protein levels 1.8-fold lower according to Western Blot quantification (Figure 5.11). The results did not show a significant difference in ADAM17 protein expression. According to our results, it is possible that the stability of ADAM17 protein was not strong and the half-life of the protein was short. Some miRNAs targeting ADAM17 mRNAs as well as ADAM17 mRNA processing could also affect the amount of ADAM17 proteins in Huh7 cells.

ADAM metallopeptidase domain 17, shortly ADAM17, is a sheddase capable of releasing the ectodomains of membrane proteins and whose substrates range from growth factors, cytokines, and receptors to many cell adhesion molecules (Scheller *et al.*, 2011). The enzyme is responsible for ectodomain shedding, in which cells can rapidly alter their surface content that subsequently triggers autocrine, paracrine, juxtacrine or endocrine signaling and responses in specific targets.

Overexpression of ADAM17 increases proliferation and invasion in breast cancer tumor samples while downregulation decreased both processes (McGowan *et al.*, 2007). Surprisingly, we detected that the mRNA level of ADAM17 in MGAT1 overexpressing Huh7 cells was lower than that of control. However, the soluble form of ADAM17 obtained from the Western Blot was not significantly different between control and MGAT1 overexpressing cells. One should know that the membrane-bound form of ADAM17 could not be detected in the SDS-PAGE of lysates prepared from the control and MGAT1 overexpressing groups since boiling of membrane proteins having high glycosylation results in aggregation of the proteins and hence no detection in the Western Blot.

We also detected physical interaction between ADAM17 and MGAT1 with the energy score of -22.18 (Figure 5.17), and MGAT1 in complex with UDP-glucose with the energy score of -6.1 (Figure 5.18). Based on this interaction, MGAT1 can be proposed as a new substrate of ADAM17, whose shedding is dependent upon ADAM17 activation. On the other hand, ADAM17 could also be a target protein for MGAT1 glycosylation process, potentially playing role in the regulation of enzyme activity *in vivo* (Chavaroche *et al.*, 2015). Both mRNA and the soluble protein levels of MGAT1 was found increased in the Wnt pathway activation (Akiva & Birgül Iyison, 2018). If we assume that ADAM17 sheddase activity acts on MGAT1 enzyme, in order to increase the amount of membrane-bound and active MGAT1, ADAM17 downregulation in MGAT1 overexpressed conditions is consistent with the tumorigenic effects of MGAT1.

Blocking IL-6 trans-signaling, in which IL-6R is a substrate of ADAM17, largely protected mice from liver cancer, suggesting that IL-6 trans-signaling was responsible for HCC. IL-6 trans-signaling was shown to be essential in promoting HCC by two distinct mechanisms: it enhances β-catenin activation and proliferation and prevents DNA-damage-induced hepatocyte apoptosis; as well as directly induces endothelial cell proliferation and subsequently promotes tumor angiogenesis (Bergmann *et al.*, 2017). So, to increase IL-6 trans-signaling, higher sheddase activity of ADAM17 which we could not observe in this study is expected in

hepatocellular carcinogenesis. Further investigations elucidating the membrane-bound ADAM17 level in the cells is needed to clarify the sheddase activity of ADAM17.

When ADAM17 mRNA and protein levels of control and MGAT1 overexpressing Huh7 cells are compared, it can be seen that even though the mRNA levels of control group was 3-fold higher than MGAT1 overexpressing group, the protein levels did not differ significantly from each other, indicating that shedding of ADAM17 (soluble form but not membrane-bound), regulated by CD9 tetraspanins (Gutiérrez-López *et al.*, 2011), is relatively higher in the control group. Further experiments investigating the levels of CD9 active form will reveal the amount of ADAM17 shedding.

The last one of the selected genes which was differentially expressed in MGAT1 overexpressing Huh7 cells was HSPA8 with Log_2FC of -2.287 in the RNA-Seq analysis. qRT-PCR results indicated the fold change as a 2.5 decrease in MGAT1 overexpressing group compared to control. The protein level of HSPA8, however, was not found significantly different between control and MGAT1 overexpressing Huh7 cells but had a 1.5-fold decrease in the latter.

Heat shock protein family A (HSP70) member 8, HSC70 or HSPA8, is a molecular chaperone which encodes a member of the heat shock protein 70 family and has a central role in many cellular processes including protection of the proteome under stress conditions, folding and refolding of proteins as well as controlling the targeting of proteins for proteolytic degradation (Bukau, Weissman, & Horwich, 2006; Lindquist & Craig, 1988).

Protein-protein interaction analysis of MGAT1 and the selected proteins that were upregulated or downregulated indicated a direct interaction between MGAT1 and HSPA8 in complex with BAG1 co-chaperone with the energy score of -16.46 (Figure 5.20). HSPA8 displays essential functions in the ubiquitin-proteasome pathway. Targeting of HSPA8 to the proteasome is provided by BAG1 co-chaperone as it interacts with both HSPA8 and the proteolytic complex

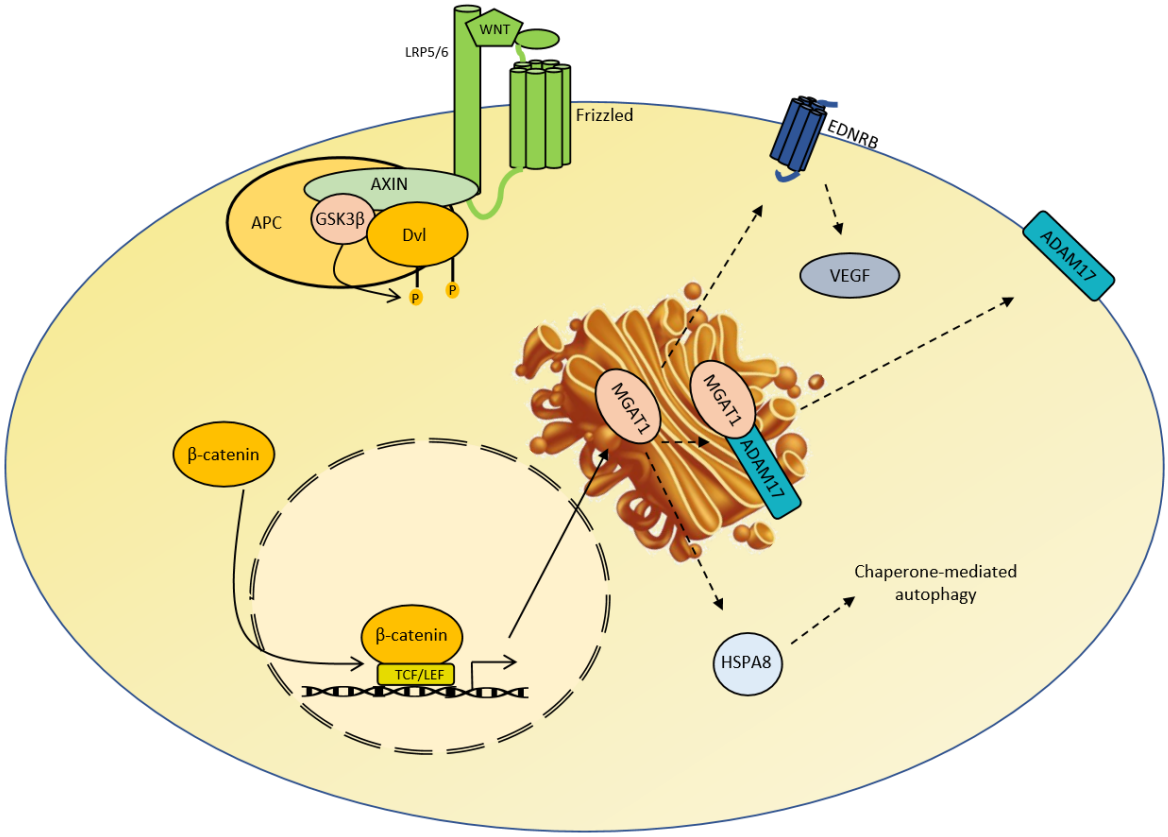

Figure 6.1. Schematic representation of the hypothesized mechanism of MGAT1 contribution to HCC.

(Lüders, Demand, & Höhfeld, 2000). HSPA8 also plays a role in the selective autophagic pathway chaperone-mediated autophagy (CMA) in which BAG1 association with HSPA8 is involved in the binding to the CMA substrates (Agarraberes & Dice, 2001). CMA upregulation has been associated with different types of cancer cells and tumors as a strategy to increase cell survival (Kon *et al.*, 2011). On the other hand, CMA has also been proposed to negatively affect some cancer types through the degradation of mutant p53 (Vakifahmetoglu-Norberg *et al.*, 2013) and hexokinase 2 (Xia *et al.*, 2015). Because cross-talks exist among different autophagy pathways, inhibition of autophagy by multiple means has been shown to promote mutant p53 degradation by inducing CMA (Vakifahmetoglu-Norberg *et al.*, 2013). HSPA8 downregulation by directly interacting with MGAT1 might be involved in the protection of mutant p53 which is a key molecule influencing many processes in cancer to increase cell survival in HCC cells.

Hepatocellular cancer is one of the deadliest cancers worldwide due to lack of knowledge of the mechanism leading to tumor formation. It is therefore crucial to investigate the underlying mechanism and develop targeted therapies to minimize the moral and economic burdens on society.

REFERENCES

Aberle, H., Bauer, A., Kispert, A., & Kemler, R. (1997). β -catenin is a target for the ubiquitin – proteasome pathway, *16*(13), 3797–3804.

Abrahamsson, A. E., Geron, I., Gotlib, J., Dao, K.-H. T., Barroga, C. F., Newton, I. G., … Jamieson, C. H. M. (2009). Glycogen synthase kinase 3 missplicing contributes to leukemia stem cell generation. *Proceedings of the National Academy of Sciences*, *106*(10), 3925–3929. https://doi.org/10.1073/pnas.0900189106

Agarraberes, F. A., & Dice, J. F. (2001). A molecular chaperone complex at the lysosomal membrane is required for protein translocation. *Journal of Cell Science*, *114*(Pt 13), 2491–2499. Retrieved from http://www.ncbi.nlm.nih.gov/pubmed/11559757

Akiva, İ. (2016). *Caracterization of Novel Wnt/β-Catenin Pathway Targets*. *Boğaziçi University*.

Akiva, I. & Birgül Iyison, N. (2018). MGAT1 is a novel transcriptional target of Wnt/β-catenin signaling pathway. *BMC Cancer*, *18*(1), 1–10. https://doi.org/10.1186/s12885-017-3960-7

Alberts, B., Johnson, A., Lewis, J., Morgan, D., Raff, M., Roberts, K., & Walter, P. (2014). *Molecular biology of the cell* (6th ed.). New York: WW Norton & Company.

Knudson, Alfred, G. (2001). Two Genetic Hits (More or less) to Cancer. *Nature Reviews Cancer*, *1*(November), 637–641.

American Cancer Society. (2018). *Cancer Facts & Figures 2018*. *American Cancer Society*.

https://doi.org/10.1182/blood-2015-12-687814

Anastas, J. N., & Moon, R. T. (2013). WNT signalling pathways as therapeutic targets in cancer. *Nature Reviews Cancer*, *13*, 11–26. https://doi.org/10.1038/nrc3419

Anguelova, E., Beuvon, F., Leonard, N., Chaverot, N., Varlet, P., Couraud, P. O., … Cazaubon, S. (2005). Functional endothelin ETB receptors are selectively expressed in human oligodendrogliomas. *Molecular Brain Research*, *137*(1–2), 77–88. https://doi.org/10.1016/j.molbrainres.2005.02.015

Azzolin, L., Panciera, T., Soligo, S., Enzo, E., Bicciato, S., Dupont, S., … Piccolo, S. (2014). YAP/TAZ incorporation in the β-catenin destruction complex orchestrates the Wnt response. *Cell*, *158*(1), 157–170. https://doi.org/10.1016/j.cell.2014.06.013

Azzolin, L., Zanconato, F., Bresolin, S., Forcato, M., Basso, G., Bicciato, S., … Piccolo, S. (2012). Role of TAZ as mediator of wnt signaling. *Cell*, *151*(7), 1443–1456. https://doi.org/10.1016/j.cell.2012.11.027

B, U. E., Mallat, A., Préaux, A., Gal, C. S., Raufaste, D., Gallois, C., … Lotersztajn, S. (1996). Growth Inhibitory Properties of Endothelin-1 in Activated Human Hepatic Stellate Cells : A Cyclic Adenosine Monophosphate – mediated Pathway Receptors, 2771–2778.

Balogh, J., Victor, D., Gordon, S., Li, X., Ghobrial, R. M., & Monsour, H. P. J. (2016). Hepatocellular carcinoma: a review. *Journal of Hepatocellular Carcinoma*, *3*, 41–53. https://doi.org/https://doi.org/10.2147/JHC.S61146

Barbier, L., Fuks, D., Pessaux, P., Muscari, F., Le Treut, Y. P., Faivre, S., & Belghiti, J. (2013). Safety of liver resection for hepatocellular carcinoma after sorafenib therapy: A multicenter case-matched study. *Annals of Surgical Oncology*, *20*(11), 3603–3609.

https://doi.org/10.1245/s10434-013-3029-z

Basu, S., Downward, J., Sudol, M., Totty, N. F., & Irwin, M. S. (2004). Akt Phosphorylates the Yes-Associated Protein, YAP, to Induce Interaction with 14-3-3 and Attenuation of p73-Mediated Apoptosis. *Molecular Cell*, *11*(1), 11–23. https://doi.org/10.1016/s1097-2765(02)00776-1

Beard, R. E., Hanto, D. W., Gautam, S., & Miksad, R. A. (2013). A comparison of surgical outcomes for noncirrhotic and cirrhotic hepatocellular carcinoma patients in a Western institution. *Surgery*, *154*(3), 545–555. https://doi.org/10.1016/j.surg.2013.02.019

Beheshti Zavareh, R., Sukhai, M. A., Hurren, R., Gronda, M., Wang, X., Simpson, C. D., … Dennis, J. W. (2012). Suppression of Cancer Progression by MGAT1 shRNA Knockdown. *PLoS ONE*, *7*(9), 4–10. https://doi.org/10.1371/journal.pone.0043721

Behrens, J., Jerchow, B. A., Wurtele, M., Grimm, J., Asbrand, C., Wirtz, R., … BIRCHMEIER, W. (1998). Functional interaction of an axin homolog, conductin, with β-catenin, APC, and GSK3β. *Science*, *280*(April), 596–599.

Behrens, J., von Kries, J. P., Kühl, M., Bruhn, L., Wedlich, D., Grosschedl, R., & Birchmeier, W. (1996). Functional interaction of β-catenin with the transcriptional factor LEF-1. *Letters to Nature*, *382*, 638–642.

Bergmann, J., Müller, M., Baumann, N., Reichert, M., Heneweer, C., Bolik, J., … Schmidt-Arras, D. (2017). IL-6 trans-signaling is essential for the development of hepatocellular carcinoma in mice. *Hepatology*, *65*(1), 89–103. https://doi.org/10.1002/hep.28874

Björklund, P., Svedlund, J., Olsson, A. K., Åkerström, G., & Westin, G. (2009). The internally truncated LRP5 receptor presents a therapeutic target in breast cancer. *PLoS ONE*, *4*(1).

https://doi.org/10.1371/journal.pone.0004243

Boyault, S., Rickman, D. S., De Reyniès, A., Balabaud, C., Rebouissou, S., Jeannot, E., … Zucman-Rossi, J. (2007). Transcriptome classification of HCC is related to gene alterations and to new therapeutic targets. *Hepatology*, *45*(1), 42–52. https://doi.org/10.1002/hep.21467

Bremnes, T., Paasche, J. D., Mehlum, A., Sandberg, C., Bremnes, B., & Attramadal, H. (2000). Regulation and intracellular trafficking pathways of the endothelin receptors. *Journal of Biological Chemistry*, *275*(23), 17596–17604. https://doi.org/10.1074/jbc.M000142200

Breous, E., & Thimme, R. (2011). Potential of immunotherapy for hepatocellular carcinoma. *Journal of Hepatology*, *54*(4), 830–834. https://doi.org/10.1016/j.jhep.2010.10.013

Bruix, J., Castells, A., Bosch, J., Feu, F., Fuster, J., Garcia-Pagan, J. C., … Rodes, J. (1996). Surgical resection of hepatocellular carcinoma in cirrhotic patients: Prognostic value of preoperative portal pressure. *Gastroenterology*, *111*(4), 1018–1022. https://doi.org/10.1016/S0016-5085(96)70070-7

Bruix, J., & Sherman, M. (2005). Management of hepatocellular carcinoma: an update. *Hepatology (Baltimore, Md.)*, *53*(3), 1020–1022. https://doi.org/10.1002/hep.24199

Buendia, M., & Neuveut, C. (2019). Hepatocellular Carcinoma. *New England Journal of Medicine*, *381*(1), e2. https://doi.org/10.1056/NEJMc1906565

Bukau, B., Weissman, J., & Horwich, A. (2006). Molecular Chaperones and Protein Quality Control. *Cell*, *125*(3), 443–451. https://doi.org/10.1016/j.cell.2006.04.014

Caja, L., Ortiz, C., Bertran, E., Murillo, M. M., Miró-Obradors, M. J., Palacios, E., & Fabregat,

I. (2007). Differential intracellular signalling induced by TGF-β in rat adult hepatocytes and hepatoma cells: Implications in liver carcinogenesis. *Cellular Signalling*, *19*(4), 683–694. https://doi.org/10.1016/j.cellsig.2006.09.002

Carter, D. A. (1997). Modulation of cellular AP-1 DNA binding activity by heat shock proteins. *FEBS Letters*, *416*(1), 81–85. https://doi.org/10.1016/S0014-5793(97)01174-5

Cavin, L. G., Venkatraman, M., Factor, V. M., Kaur, S., Schroeder, I., Mercurio, F., … Arsura, M. (2004). Regulation of α-fetoprotein by nuclear factor-κB protects hepatocytes from tumor necrosis factor-α cytotoxicity during fetal liver development and hepatic oncogenesis. *Cancer Research*, *64*(19), 7030–7038. https://doi.org/10.1158/0008-5472.CAN-04-1647

Chairoungdua, A., Smith, D. L., Pochard, P., Hull, M., & Caplan, M. J. (2010). Exosome release of β-catenin: A novel mechanism that antagonizes Wnt signaling. *Journal of Cell Biology*, *190*(6), 1079–1091. https://doi.org/10.1083/jcb.201002049

Chan, E. H. Y., Nousiainen, M., Chalamalasetty, R. B., Schäfer, A., Nigg, E. A., & Sillje, H. H. W. (2005). The Ste20-like kinase Mst2 activates the human large tumor suppressor kinase Lats1. *Oncogene*, *24*(12), 2076–2086. https://doi.org/10.1038/sj.onc.1208445

Chantôme, A., Pance, A., Gauthier, N., Vandroux, D., Chenu, J., Solary, E., … Reveneau, S. (2004). Casein kinase II-mediated phosphorylation of NF-κB p65 subunit enhances inducible nitric-oxide synthase gene transcription in vivo. *Journal of Biological Chemistry*, *279*(23), 23953–23960. https://doi.org/10.1074/jbc.M313731200

Chavaroche, A., Cudic, M., Giulianotti, M., Houghten, R. A., Fields, G. B., & Minond, D. (2015). Glycosylation of A Disintegrin And Metalloprotease 17 (ADAM17) Affects its Activity and Inhibition, *15*(449), 68–75. https://doi.org/10.1016/j.ab.2013.12.018.Glycosylation

Chen, D., Lin, X., Zhang, C., An, G., Li, Z., Dong, B., … Zhang, X. (2019). Activated wnt signaling promotes growth and progression of afp-producing gastric cancer in preclinical models. *Cancer Management and Research*, *11*, 1349–1362. https://doi.org/10.2147/CMAR.S187219

Chiang, D. Y., Villanueva, A., Hoshida, Y., Peix, J., Newell, P., Sole, M., … Azra. (2008). Focal Gains of Vascular Endothelial Growth Factor A and Molecular Classification of Hepatocellular Carcinoma. *Cancer Res.*, *15*(68), 6779–6788. https://doi.org/10.1371/journal.pone.0178059

Chuang, S. C., Vecchia, C. La, & Boffetta, P. (2009). Liver cancer: Descriptive epidemiology and risk factors other than HBV and HCV infection. *Cancer Letters*, *286*(1), 9–14. https://doi.org/10.1016/j.canlet.2008.10.040

Cieply, B., Zeng, G., Proverbs-Singh, T., Geller, D. A., & Monga, S. P. S. (2009). Unique Phenotype of Hepatocellular Cancers with Exon-3 Mutations in Beta-catenin Gene. *Hepatology*, *49*(3), 821–831.

Cleary, S. P., Jeck, W. R., Zhao, X., Chen, K., Selitsky, S. R., Savich, G. L., … Ghanekar, A. (2013). Identification of Driver Genes in Hepatocellular Carcinoma by Exome Sequencing. *Hepatology*, *58*(5), 1693–1702. https://doi.org/10.1371/journal.pone.0178059

Clevers, H. (2006). *Wnt /β-Catenin Signaling in Development and Disease*. *Cell* (Vol. 127). https://doi.org/10.1016/j.cell.2006.10.018

Clinkenbeard, E. L., Butler, J. E., & Spear, B. T. (2012). Pericentral activity of AFP enhancer E3 and glutamine synthetase upstream enhancer in the adult liver are regulated by β-catenin. *Bone*, *56*(5), 1892–1901. https://doi.org/10.1038/jid.2014.371

Conlon, I., & Raff, M. (1999). Size control in animal development. *Cell*, *96*(2), 235–244. https://doi.org/10.1016/S0092-8674(00)80563-2

Cooper, G. M., & Haussman, R. E. (2009). *The Cell: A Molecular Approach*. Washington D.C.: ASM Press.

Dauphinée, M. J., & Mizejewski, G. J. (2002). Human alpha-fetoprotein contains potential heterodimerization motifs capable of interaction with nuclear receptors and transcription/growth factors. *Medical Hypotheses*, *58*(6), 453–461. https://doi.org/10.1054/mehy.2001.1445

Demunter, A., De Wolf-Peeters, C., Degreef, H., Stas, M., & Van Den Oord, J. J. (2001). Expression of the endothelin-B receptor in pigment cell lesions of the skin: Evidence for its role as tumor progression marker in malignant melanoma. *Virchows Archiv*, *438*(5), 485–491. https://doi.org/10.1007/s004280000362

Densham, R. M., O'Neill, E., Munro, J., Konig, I., Anderson, K., Kolch, W., & Olson, M. F. (2009). MST Kinases Monitor Actin Cytoskeletal Integrity and Signal via c-Jun N-Terminal Kinase Stress-Activated Kinase To Regulate p21Waf1/Cip1 Stability. *Molecular and Cellular Biology*, *29*(24), 6380–6390. https://doi.org/10.1128/mcb.00116-09

Dominguez, I., Sonenshein, G. E., & Seldin, D. C. (2009). CK2 and its role in Wnt and NF-κB signaling: Linking development and cancer. *Cellular and Molecular Life Sciences*, *66*(11–12), 1850–1857. https://doi.org/10.1007/s00018-009-9153-z

Dong, J., Feldmann, G., Huang, J., Wu, S., Zhang, N., Comerford, S. A., … Pan, D. (2007). Elucidation of a Universal Size-Control Mechanism in Drosophila and Mammals. *Cell*, *130*(6), 1120–1133. https://doi.org/10.1016/j.cell.2007.07.019

Edamoto, Y., Hara, A., Biernat, W., Terracciano, L., Cathomas, G., Riehle, H. M., … Ohgaki, H. (2003). Alterations of RB1, p53 and Wnt pathways in hepatocellular carcinomas associated with hepatitis C, hepatitis B and alcoholic liver cirrhosis. *International Journal of Cancer*, *106*(3), 334–341. https://doi.org/10.1002/ijc.11254

Eddy, S. F., Guo, S., Demicco, E. G., Romieu-Mourez, R., Landesman-Bollag, E., Seldin, D. C., & Sonenshein, G. E. (2005). Inducible IκB kinase/IκB kinase ε expression is induced by CK2 and promotes aberrant nuclear factor-κB activation in breast cancer cells. *Cancer Research*, *65*(24), 11375–11383. https://doi.org/10.1158/0008-5472.CAN-05-1602

Egeblad, M., Rasch, M. G., & Weaver, V. M. (2010). Dynamic interplay between the collagen scaffold and tumor evolution. *Current Opinion in Genetics and Development*, *22*(5), 697–706. https://doi.org/10.1016/j.ceb.2010.08.015.Dynamic

El-Serag, H. B., Marrero, J. A., Rudolph, L., & Reddy, K. R. (2008). Diagnosis and Treatment of Hepatocellular Carcinoma. *Gastroenterology*, *134*(6), 1752–1763. https://doi.org/10.1053/j.gastro.2008.02.090

Endo, K., Ueda, T., Ueyama, J., Ohta, T., & Terada, T. (2000). Immunoreactive E-cadherin, alpha-catenin, beta-catenin, and gamma- catenin proteins in hepatocellular carcinoma: Relationships with tumor grade, clinicopathologic parameters, and patients' survival. *Human Pathology*, *31*(5), 558–565. https://doi.org/10.1053/hp.2000.6683

Ferenci, P., Fried, M., Labrecque, D., Bruix, J., Sherman, M., Omata, M., … Mair, A. Le. (2010). Hepatocellular carcinoma (HCC): a global perspective. *Arab Journal of Gastroenterology*, *11*(3), 174–179. https://doi.org/10.1016/j.ajg.2010.04.001

Ferlay, J., Shin, H.-R., Bray, F., Forman, D., Mathers, C., & Parkin, D. M. (2010). Estimates of worldwide burden of cancer in 2008: GLOBOCAN 2008. *International Journal of Cancer*, *127*(12), 2893–2917. https://doi.org/10.1002/ijc.25516

Gao, F., Zhu, H. K., Zhu, Y. B., Shan, Q. N., Ling, Q., Wei, X. Y., … Zheng, S. Sen. (2016). Predictive value of tumor markers in patients with recurrent hepatocellular carcinoma in different vascular invasion pattern. *Hepatobiliary and Pancreatic Diseases International*, *15*(4), 371–377. https://doi.org/10.1016/S1499-3872(16)60095-4

Genevet, A., & Tapon, N. (2011). The Hippo pathway and apico–basal cell polarity. *Biochemical Journal*, *436*(2), 213–224. https://doi.org/10.1042/bj20110217

Giles, R. H., Van Es, J. H., & Clevers, H. (2003). Caught up in a Wnt storm: Wnt signaling in cancer. *Biochimica et Biophysica Acta - Reviews on Cancer*, *1653*(1), 1–24. https://doi.org/10.1016/S0304-419X(03)00005-2

Guichard, C., Amaddeo, G., Imbeaud, S., Ladeiro, Y., Pelletier, L., Maad, I. Ben, … Zucman-Rossi, J. (2012). Integrated analysis of somatic mutations and focal copy-number changes identifies key genes and pathways in hepatocellular carcinoma. *Nature Genetics*, *44*(6), 694–698. https://doi.org/10.1038/ng.2256

Guo, D., Zhang, H., Tan, S., & Gu, Y. (2014). Nifedipine Promotes the Proliferation and Migration of Breast Cancer Cells. *PLoS ONE*, *9*(12), e113649. https://doi.org/10.1371/journal.pone.0113649

Gusella, J. F., Ramesh, V., MacCollin, M., & Jacoby, L. B. (1999). Merlin: The neurofibromatosis 2 tumor suppressor. *Biochimica et Biophysica Acta - Reviews on Cancer*, *1423*(2). https://doi.org/10.1016/S0304-419X(99)00005-0

Gutiérrez-López, M. D., Gilsanz, A., Yàñez-Mó, M., Ovalle, S., Lafuente, E. M., Domínguez, C., … Cabañas, C. (2011). The sheddase activity of ADAM17/TACE is regulated by the tetraspanin CD9. *Cellular and Molecular Life Sciences*, *68*(19), 3275–3292. https://doi.org/10.1007/s00018-011-0639-0

Halder, G., & Johnson, R. L. (2011). Hippo signaling: growth control and beyond. *Development*, *138*(1), 9–22. https://doi.org/10.1242/dev.045500

Hamilton, G., Yee, K. S., Scrace, S., & Neill, E. O. (2009). ATM Regulates a RASSF1A-Dependent DNA Damage Response. *Current Biology*, *19*(23), 2020–2025. https://doi.org/10.1016/j.cub.2009.10.040.ATM

Hanahan, D., & Weinberg, R. A. (2011). Hallmarks of Cancer: The Next Generation. *Cell*, *144*(5), 646–674. https://doi.org/10.1016/j.cell.2011.02.013

Harvey, K. F., Zhang, X., & Thomas, D. M. (2013). The Hippo pathway and human cancer. *Nature Reviews Cancer*, *13*(4), 246–257. https://doi.org/10.1038/nrc3458

Herbst, D. A., & Reddy, K. R. (2011). Risk factors for hepatocellular carcinoma. *Archives of Hellenic Medicine*, *1*(6), 180–182. https://doi.org/10.4172/1948-5956.S17-009

Hessvik, N. P., & Llorente, A. (2018). Current knowledge on exosome biogenesis and release. *Cellular and Molecular Life Sciences*, *75*(2), 193–208. https://doi.org/10.1007/s00018-017-2595-9

Houessinon, A., Gicquel, A., Bochereau, F., Louandre, C., Nyga, R., Godin, C., … Galmiche, A. (2016). Alpha-fetoprotein is a biomarker of unfolded protein response and altered proteostasis in hepatocellular carcinoma cells exposed to sorafenib. *Cancer Letters*, *370*(2), 242–249. https://doi.org/10.1016/j.canlet.2015.10.032

Huber, A. H., Nelson, W. J., & Weis, W. I. (1997). Three-Dimensional Structure of the Armadillo Repeat Region of β-Catenin. *Cell*, *90*, 871–882.

Ikeda, S., Kishida, S., Yamamoto, H., Murai, H., Koyama, S., & Kikuchi, A. (1998). Axin, a

negative regulator of the Wnt signaling pathway, forms a complex with GSK-3β and. *The EMBO Journal*, *17*(5), 1371–1384. https://doi.org/10.1093/emboj/16.13.3797

Inagawa, S., Adachi, S., Kawamoto, T., Fukao, K., Itabashi, M., Hori, M., … Yoshimi, F. (2002). Expression and prognostic roles of β-catenin in hepatocellular carcinoma: Correlation with tumor progression and postoperative survival. *Clinical Cancer Research*, *8*(2), 450–456.

Ioffe, E., Liu, Y., & Stanley, P. (1997). Complex N-glycans in Mgat1 null preimplantation embryos arise from maternal Mgat1 RNA. *Glycobiology*, *7*(7), 913–919. https://doi.org/10.1093/glycob/7.7.913

Jamora, C., & Fuchs, E. (2002). Intercellular adhesion, signalling and the cytoskeleton. *Nature Cell Biology*, *4*, 101–108. https://doi.org/10.1038/ncb0402-e101

Jesmin, S., Miyauchi, T., Goto, K., & Yamaguchi, I. (2006). Down-regulated VEGF expression in the diabetic heart is normalized by an endothelin ETA receptor antagonist. *European Journal of Pharmacology*, *541*(1–2), 184–185. https://doi.org/10.1016/j.ejphar.2006.04.041

Jhunjhunwala, S., Jiang, Z., Stawiski, E. W., Gnad, F., Liu, J., Mayba, O., … Zhang, Z. (2014). Diverse modes of genomic alteration in hepatocellular carcinoma. *Genome Biology*, *15*(8), 436. https://doi.org/10.1186/s13059-014-0436-9

Justice, R. W., Zilian, O., Woods, D. F., Noll, M., & Bryant, P. J. (1995). The Drosophila tumor suppressor gene warts encodes a homolog of human myotonic dystrophy kinase and is required for the control of cell shape and proliferation. *Genes and Development*, *9*(5), 534–546. https://doi.org/10.1101/gad.9.5.534

Kahn, M. (2014). Can we safely target the WNT pathway? *Nature Review Drug Discovery*, *13*(7), 513–532. https://doi.org/110.1016/j.bbi.2017.04.008

Kato, T., Shingo Kameoka, Kimura, T., Soga, N., Abe, Y., Nishikawa, T., & Kobayashi, M. (2001). Angiogenesis as a predictor of long-term survival for 377 Japanese patients with breast cancer. *Breast Cancer Research and Treatment*, *70*(1), 65–74. https://doi.org/10.1023/A:1012534724488

Kavak, E., Najafov, A., Ozturk, N., Seker, T., Cavusoglu, K., Aslan, T., … Koman, A. (2010). Analysis of the Wnt/B-catenin/TCF4 pathway using SAGE, genome-wide microarray and promoter analysis: Identification of BRI3 and HSF2 as novel targets. *Cellular Signalling*, *22*(10), 1523–1535. https://doi.org/10.1016/j.cellsig.2010.05.021

Khokhlatchev, A., Rabizadeh, S., Xavier, R., Nedwidek, M., Chen, T., Zhang, X. F., … Avruch, J. (2002). Identification of a novel Ras-regulated proapoptotic pathway. *Current Biology*, *12*(4), 253–265. https://doi.org/10.1016/S0960-9822(02)00683-8

Kon, M., Kiffin, R., Koga, H., Chapochnick, J., Macian, F., Varticovski, L., & Cuervo, A. M. (2011). Chaperone-mediated autophagy is required for tumor growth. *Science Translational Medicine*, *3*(109), 1–30. https://doi.org/10.1126/scitranslmed.3003182

Lahav, R. (2005). Endothelin receptor B is required for the expansion of melanocyte precursors and malignant melanoma. *International Journal of Developmental Biology*, *49*(2–3 SPEC. ISS.), 173–180. https://doi.org/10.1387/ijdb.041951rl

Lahav, R., Heffner, G., & Patterson, P. H. (1999). An endothelin receptor B antagonist inhibits growth and induces cell death in human melanoma cells in vitro and in vivo. *Proceedings of the National Academy of Sciences*, *96*(20), 11496–11500. https://doi.org/10.1073/pnas.96.20.11496

Lammi, L., Sirpa Arte, Somer, M., Jarvinen, H., Lahermo, P., Thesleff, I., … Nieminen, P. (2004). Mutations in AXIN2 Cause Familial Tooth Agenesis and Predispose to Colorectal Cancer. *American Journal of Human Genetics*, *74*, 1043–1050.

Lee, H. C., Kim, M., & Wands, J. R. (2006). Wnt/frizzled signaling in hepatocellular carcinoma. *Frontiers in Bioscience*, *11*, 1901–1915. https://doi.org/10.2741/1933

Lei, Q.-Y., Zhang, H., Zhao, B., Zha, Z.-Y., Bai, F., Pei, X.-H., … Guan, K.-L. (2008). TAZ Promotes Cell Proliferation and Epithelial-Mesenchymal Transition and Is Inhibited by the Hippo Pathway. *Molecular and Cellular Biology*, *28*(7), 2426–2436. https://doi.org/10.1128/mcb.01874-07

Li, J., Chen, X., Ding, X., Cheng, Y., Zhao, B., Lai, Z., … Wang, C.-Y. (2013). LATS2 Suppresses Oncogenic Wnt Signaling by Disrupting β- catenin/BCL9 Interaction, *5*(6), 1650–1663. https://doi.org/10.1016/j.celrep.2013.11.037.

Li, M., Zhou, S., Liu, X., Li, P., McNutt, M. A., & Li, G. (2007). α-Fetoprotein shields hepatocellular carcinoma cells from apoptosis induced by tumor necrosis factor-related apoptosis-inducing ligand. *Cancer Letters*, *249*(2), 227–234. https://doi.org/10.1016/j.canlet.2006.09.004

Lindquist, S., & Craig, E. A. (1988). The heat-shock proteins, *22*, 631–677.

Liu, C. Y., Zha, Z. Y., Zhou, X., Zhang, H., Huang, W., Zhao, D., … Guan, K. L. (2010). The hippo tumor pathway promotes TAZ degradation by phosphorylating a phosphodegron and recruiting the SCFβ-TrCP E3 ligase. *Journal of Biological Chemistry*, *285*(48), 37159–37169. https://doi.org/10.1074/jbc.M110.152942

Liu, J., Zhu, G., Jia, N., Wang, W., Wang, Y., Yin, M., … Zhang, J. (2019). CD9 regulates

keratinocyte migration by negatively modulating the sheddase activity of ADAM17. *International Journal of Biological Sciences*, *15*(2), 493–506. https://doi.org/10.7150/ijbs.29404

Llovet, J. M., Villanueva, A., Lachenmayer, A., & Finn, R. S. (2015). Advances in targeted therapies for hepatocellular carcinoma in the genomic era. *Nature Reviews Clinical Oncology*, *12*(7), 408–424. https://doi.org/10.1038/nrclinonc.2015.103

Logan, C. Y., & Nusse, R. (2004). The Wnt Signaling Pathway in Development and Disease. *Annual Review of Cell and Developmental Biology*, *20*(1), 781–810. https://doi.org/10.1146/annurev.cellbio.20.010403.113126

Lüders, J., Demand, J., & Höhfeld, J. (2000). The ubiquitin-related BAG-1 provides a link between the molecular chaperones Hsc70/Hsp70 and the proteasome. *Journal of Biological Chemistry*, *275*(7), 4613–4617. https://doi.org/10.1074/jbc.275.7.4613

Luedde, T., & Schwabe, R. F. (2011). NFkB in the liver-linking injury, fibrosis and hepatocellular carcinoma. *Nat Rev Gastroenterol Hepatol*, *8*(2), 108–118. https://doi.org/10.1038/nrgastro.2010.213.NF-

Marvin, M. L., Mazzoni, S. M., Herron, C. M., Edwards, S., Gruber, S. B., & Petty, E. M. (2011). AXIN2-associated autosomal dominant ectodermal dysplasia and neoplastic syndrome. *American Journal of Medical Genetics, Part A*, *155*(4), 898–902. https://doi.org/10.1002/ajmg.a.33927

McGowan, P. M., Ryan, B. M., Hill, A. D. K., McDermott, E., O'Higgins, N., & Duffy, M. J. (2007). ADAM-17 expression in breast cancer correlates with variables of tumor progression. *Clinical Cancer Research*, *13*(8), 2335–2343. https://doi.org/10.1158/1078-0432.CCR-06-2092

Merle, P., Kim, M., Herrmann, M., Gupte, A., Lefrançois, L., Califano, S., … Wands, J. R. (2005). Oncogenic role of the frizzled-7/β-catenin pathway in hepatocellular carcinoma. *Journal of Hepatology*, *43*(5), 854–862. https://doi.org/10.1016/j.jhep.2005.05.018

Molenaar, M., Wetering, M. Van De, Oosterwegel, M., Peterson-maduro, J., Godsave, S., Korinek, V., & Roose, J. (1996). XTcf-3 Transcription Factor Mediates β-Catenin-Induced Axis Formation in Xenopus Embryos. *Cell*, *86*, 391–399.

Muehlemann, M., Miller, K. D., Dauphinee, M., & Mizejewski, G. J. (2005). Review of Growth Inhibitory Peptide as a Biotherapeutic agent for tumor growth, adhesion, and metastasis. *Cancer and Metastasis Reviews*, *24*(3), 441–467. https://doi.org/10.1007/s10555-005-5135-2

Nejak-Bowen, K., Kikuchi, A., & Monga, S. P. S. (2013). Beta-catenin-NF-κB interactions in murine hepatocytes: A complex to die for, *57*(2), 763–774.

Nelson, J., Bagnato, A., Battistini, B., & Nisen, P. (2003). The endothelin axis: Emerging role in cancer. *Nature Reviews Cancer*, *3*(2), 110–116. https://doi.org/10.1038/nrc990

Ota, M., & Sasaki, H. (2008). Mammalian Tead proteins regulate cell proliferation and contact inhibition as transcriptional mediators of Hippo signaling. *Development*, *135*(24), 4059–4069. https://doi.org/10.1242/dev.027151

Pallares, J., Llobet, D., Santacana, M., Eritja, N., Velasco, A., Cuevas, D., … Matias-Guiu, X. (2009). CK2β is expressed in endometrial carcinoma and has a role in apoptosis resistance and cell proliferation. *American Journal of Pathology*, *174*(1), 287–296. https://doi.org/10.2353/ajpath.2009.080552

Perz, J. F., Armstrong, G. L., Farrington, L. A., Hutin, Y. J. F., & Bell, B. P. (2006). The

contributions of hepatitis B virus and hepatitis C virus infections to cirrhosis and primary liver cancer worldwide. *Journal of Hepatology*, *45*(4), 529–538. https://doi.org/10.1016/j.jhep.2006.05.013

Piccolo, S., Dupont, S., & Cordenonsi, M. (2014). The Biology of YAP/TAZ: Hippo Signaling and Beyond. *Physiological Reviews*, *94*(4), 1287–1312. https://doi.org/10.1152/physrev.00005.2014

Pinna, L. A. (2002). Protein kinase CK2: a challenge to canons. *Journal of Cell Science*, *115*(Pt 20), 3873–3878. https://doi.org/10.1242/jcs.00074

Polakis, P. (2007). The many ways of Wnt in cancer. *Current Opinion in Genetics and Development*, *17*(1), 45–51. https://doi.org/10.1016/j.gde.2006.12.007

Polakis, P. (2012). Wnt signaling in Cancer | The Wnt Homepage. *Cold Spring Harb Perspect Biol.*, *4*(5), a008052.

Polesel, J., Zucchetto, A., Montella, M., Dal Maso, L., Crispo, A., La Vecchia, C., … Talamini, R. (2009). The impact of obesity and diabetes mellitus on the risk of hepatocellular carcinoma. *Annals of Oncology*, *20*(2), 353–357. https://doi.org/10.1093/annonc/mdn565

Praskova, M., Xia, F., & Avruch, J. (2008). MOBKL1A/MOBKL1B Phosphorylation by MST1 and MST2 Inhibits Cell Proliferation. *Current Biology*, *18*(5), 311–321. https://doi.org/10.1016/j.cub.2008.02.006

Romieu-Mourez, R. (2001). Roles of IKK kinases and protein kinase CK2 in activation of NF-[kappa]B in breast cancer. *Cancer Res.*, *61*, 3810–3818.

Rowland, B. D., & Peeper, D. S. (2006). KLF4, p21 and context-dependent opposing forces in

cancer. *Nature Reviews Cancer*, *6*(1), 11–23. https://doi.org/10.1038/nrc1780

S. R. Hamilton, L. A. A. (2001). Pathology and Genetics of Tumours of the Digestive System (Vol. 38, pp. 179–180).

Sahin, U., Weskamp, G., Kelly, K., Zhou, H. M., Higashiyama, S., Peschon, J., … Blobel, C. P. (2004). Distinct roles for ADAM10 and ADAM17 in ectodomain shedding of six EGFR ligands. *Journal of Cell Biology*, *164*(5), 769–779. https://doi.org/10.1083/jcb.200307137

Salahshor, S., & Woodgett, J. R. (2005). The links between axin and carcinogenesis. *Journal of Clinical Pathology*, *58*(3), 225–236. https://doi.org/10.1136/jcp.2003.009506

Salani, D., Rosanò, L., Castro, V. Di, Bagnato, A., Taraboletti, G., Borsotti, P., & Giavazzi, R. (2000). Endothelin-1 induces an angiogenic phenotype in cultured endothelial cells and stimulates neovascularization in vivo. *American Journal of Pathology*, *157*(5), 1703–1711. https://doi.org/10.1016/S0002-9440(10)64807-9

Scheller, J., Chalaris, A., Garbers, C., & Rose-John, S. (2011). ADAM17: A molecular switch to control inflammation and tissue regeneration. *Trends in Immunology*, *32*(8), 380–387. https://doi.org/10.1016/j.it.2011.05.005

Schulze, K., Imbeaud, S., Letouzé, E., Ludmil, B., & Ligue, E. L. (2015). Exome sequencing of hepatocellular carcinomas identifies new mutational signatures and potential therapeutic targets, *47*(5), 505–511. https://doi.org/10.1038/ng.3252.Exome

Sebastian, A., Hum, N. R., Murugesh, D. K., Hatsell, S., Economides, A. N., & Loots, G. G. (2017). Wnt co-receptors Lrp5 and Lrp6 differentially mediate Wnt3a signaling in osteoblasts. *PLoS ONE*, *12*(11), 1–19. https://doi.org/10.1371/journal.pone.0188264

Seldin, D. C., & Landesman-Bollag, E. (2013). The oncogenic potential of CK2. In L. A. Pinna (Ed.), *Protein Kinase CK2* (pp. 294–304). Oxford U.K.: Wiley-Blackwell.

Seldin, D. C., Landesman-Bollag, E., Farago, M., Currier, N., Lou, D., & Dominguez, I. (2005). CK2 as a positive regulator of Wnt signalling and tumourigenesis. *Molecular and Cellular Biochemistry*, *274*(1–2), 63–67. https://doi.org/10.1007/s11010-005-3078-0

Sheikh, M. Y., Choi, J., Qadri, I., Friedman, J. E., & Sanyal, A. J. (2008). Hepatitis C virus infection: Molecular pathways to metabolic syndrome. *Hepatology*, *47*(6), 2127–2133. https://doi.org/10.1002/hep.22269

Shi, C., Cai, Y., Li, Y., Li, Y., Hu, N., Ma, S., … Zhou, H. (2018). Yap promotes hepatocellular carcinoma metastasis and mobilization via governing cofilin/F-actin/lamellipodium axis by regulation of JNK/Bnip3/SERCA/CaMKII pathways. *Redox Biology*, *14*(July 2017), 59–71. https://doi.org/10.1016/j.redox.2017.08.013

Siew, W. C., Chun, J. L., Guo, K., Chee, P. N., Lee, I., Hunziker, W., … Hong, W. (2008). A role for TAZ in migration, invasion, and tumorigenesis of breast cancer cells. *Cancer Research*, *68*(8), 2592–2598. https://doi.org/10.1158/0008-5472.CAN-07-2696

Song, D. H., Sussman, D. J., & Seldin, D. C. (2000). Endogenous protein kinase CK2 participates Wnt signaling in mammary epithelial cells. *Journal of Biological Chemistry*, *275*(31), 23790–23797. https://doi.org/10.1074/jbc.M909107199

Sun, H., Gao, Y., Lu, K., Zhao, G., Li, X., Li, Z., & Chang, H. (2015). Overexpression of Klotho suppresses liver cancer progression and induces cell apoptosis by negatively regulating wnt/β-catenin signaling pathway. *World Journal of Surgical Oncology*, *13*(1), 1–8. https://doi.org/10.1186/s12957-015-0717-0

Szabó, E., Páska, C., Kaposi Novák, P., Schaff, Z., & Kiss, A. (2004). Similarities and Differences in Hepatitis B and C Virus Induced Hepatocarcinogenesis. *Pathology and Oncology Research*, *10*(1), 5–11. https://doi.org/10.1007/BF02893401

Szklarczyk, D., Gable, A. L., Lyon, D., Junge, A., Wyder, S., Huerta-Cepas, J., … Von Mering, C. (2018). STRING v11: Protein-protein association networks with increased coverage, supporting functional discovery in genome-wide experimental datasets. *Nucleic Acids Research*, *47*(D1), D607–D613. https://doi.org/10.1093/nar/gky1131

Thorgeirsson, S. S., & Grisham, J. W. (2002). Molecular pathogenesis of hepatocellular carcinoma. *Nature Genetics*, *31*, 339–346. https://doi.org/10.1159/000449340

Uhl, P., Fricker, G., Haberkorn, U., & Mier, W. (2014). Current status in the therapy of liver diseases. *International Journal of Molecular Sciences*, *15*(5), 7500–7512. https://doi.org/10.3390/ijms15057500

Vakifahmetoglu-Norberg, H., Kim, M., Xia, H. guang, Iwanicki, M. P., Ofengeim, D., Coloff, J. L., … Yuan, J. (2013). Chaperone-mediated autophagy degrades mutant p53. *Genes and Development*, *27*(15), 1718–1730. https://doi.org/10.1101/gad.220897.113

Wada, K.-I., Itoga, K., Okano, T., Yonemura, S., & Sasaki, H. (2011). Hippo pathway regulation by cell morphology and stress fibers. *Development*, *138*(18), 3907–3914. https://doi.org/10.1242/dev.070987

Waly Raphael, S., Yangde, Z., & YuXiang, C. (2012). Hepatocellular Carcinoma: Focus on Different Aspects of Management. *ISRN Oncology*, *2012*, 1–12. https://doi.org/10.5402/2012/421673

Wang, D., Westerheide, S. D., Hanson, J. L., & Baldwin, J. (2000). Tumor necrosis factor α-

induced phosphorylation of RelA/p65 on Ser529 is controlled by casein kinase II. *Journal of Biological Chemistry*, *275*(42), 32592–32597. https://doi.org/10.1074/jbc.M001358200

Wang, Y., Han, C., Lu, L., Magliato, S., & Wu, T. (2013). Hedgehog Signaling Pathway Regulates Autophagy in Human Hepatocellular Carcinoma Cell. *Hepatology*, *58*(3), 1995–1010.

Wilhelm, S. M., Dumas, J., Adnane, L., Lynch, M., Carter, C. A., Schütz, G., … Zopf, D. (2011). Regorafenib (BAY 73-4506): A new oral multikinase inhibitor of angiogenic, stromal and oncogenic receptor tyrosine kinases with potent preclinical antitumor activity. *International Journal of Cancer*, *129*(1), 245–255. https://doi.org/10.1002/ijc.25864

Wong, C. M., Fan, S. T., & Ng, I. O. L. (2001). B-Catenin Mutation and Overexpression in Hepatocellular Carcinoma. *Cancer*, *92*(1), 136–145. https://doi.org/10.1002/1097-0142(20010701)92:1<136::aid-cncr1301>3.0.co;2-r

World Health Organization. (2018). Cancer.

Wu, H., Liu, G., Li, C., & Zhao, S. (2003). Bri3, a Novel Gene, Participates in Tumor Necrosis Factor-A-Induced Cell Death. *Biochemical and Biophysical Research Communications*, *311*(2), 518–524. https://doi.org/10.1016/j.bbrc.2003.10.038

Xia, H. guang, Najafov, A., Geng, J., Galan-Acosta, L., Han, X., Guo, Y., … Vakifahmetoglu-Norberg, H. (2015). Degradation of HK2 by chaperone-mediated autophagy promotes metabolic catastrophe and cell death. *Journal of Cell Biology*, *210*(5), 705–716. https://doi.org/10.1083/jcb.201503044

Xu, Y., Stamenkovic, I., & Yu, Q. (2010). CD44 attenuates activation of the Hippo signaling pathway and is a prime therapeutic target for glioblastoma. *Cancer Research*, *70*(6), 2455–

2464. https://doi.org/10.1158/0008-5472.CAN-09-2505

Yimlamai, D., Fowl, B. H., & Camargo, F. D. (2015). Emerging evidence on the role of the Hippo/YAP pathway in liver physiology and cancer. *Journal of Hepatology*, *63*(6), 1491–1501. https://doi.org/10.1016/j.jhep.2015.07.008

Yip, B., Chen, S.-H., Mulder, H., Höppener, J. W. M., & Schachter, H. (1997). Organization of the human β-1,2-N-acetylglucosaminyltransferase I gene (MGAT1), which controls complex and hybrid N-glycan synthesis. *Biochemical Journal*, *321*(2), 465–474. https://doi.org/10.1042/bj3210465

Yost, C., Torres, M., Miller, J. R., Huang, E., Kimelman, D., & Moon, R. T. (1996). The axis-inducing activity, stability, and subcellular distribution of β-catenin is regulated in Xenopus embryos by glycogen synthase 3. *Genes and Development*, (10), 1443–1454.

Yu, F.-X., Zhao, B., Panupinthu, N., Jewell, J. L., Lian, I., Wang, L. H., … Guan, K.-L. (2012). Regulation of the Hippo-YAP pathway by G-protein coupled receptor signaling. *Cell*, *150*(4), 780–791. https://doi.org/10.1371/journal.pone.0178059

Yu, F. X., Zhao, B., Panupinthu, N., Jewell, J. L., Lian, I., Wang, L. H., … Guan, K. L. (2012). Regulation of the Hippo-YAP pathway by G-protein-coupled receptor signaling. *Cell*, *150*(4), 780–791. https://doi.org/10.1016/j.cell.2012.06.037

Yuan, M., Tomlinson, V., Lara, R., Holliday, D., Chelala, C., Harada, T., … Basu, S. (2008). Yes-associated protein (YAP) functions as a tumor suppressor in breast. *Cell Death and Differentiation*, *15*(11), 1752–1759. https://doi.org/10.1038/cdd.2008.108

Zhang, H., Wang, X., & Chen, X. (2017). Potential role of long non-coding RNA ANRIL in pediatric medulloblastoma through promotion on proliferation and migration by targeting

miR-323. *Journal of Cellular Biochemistry*. https://doi.org/10.1002/jcb.26141

Zhang, Y.-Y., & Feng, H.-M. (2017). MEG3 Suppresses Human Pancreatic Neuroendocrine Tumor Cells Growth and Metastasis by Down-Regulation of Mir-183. *Cellular Physiology and Biochemistry*, *44*, 345–356. https://doi.org/10.1159/000484906

Zhao, B., Li, L., Tumaneng, K., Wang, C. Y., & Guan, K. L. (2010). A coordinated phosphorylation by Lats and CK1 regulates YAP stability through SCFβ-TRCP. *Genes and Development*, *24*(1), 72–85. https://doi.org/10.1101/gad.1843810

Zhao, B., Li, L., Wang, L., Wang, C. Y., Yu, J., & Guan, K. L. (2012). Cell detachment activates the Hippo pathway via cytoskeleton reorganization to induce anoikis. *Genes and Development*, *26*(1), 54–68. https://doi.org/10.1101/gad.173435.111

Zhao, B., Ye, X., Yu, J., Li, L., Li, W., Li, S., … Guan, K. L. (2008). TEAD mediates YAP-dependent gene induction and growth control. *Genes and Development*, *22*(14), 1962–1971. https://doi.org/10.1101/gad.1664408

Zhao, B., Zhao, B., Wei, X., Wei, X., Li, W., Li, W., … Guan, K. (2007). Inactivation of YAP oncoprotein by the Hippo pathway is involved in cell contact inhibition and tissue growth control. *Genes and Development*, *21*, 2747–2761. https://doi.org/10.1101/gad.1602907.Hpo/Sav

Zhou, D., Conrad, C., Xia, F., Park, J.-S., Payer, B., Yin, Y., … Avruch, J. (2009). Mst1 and Mst2 maintain hepatocyte quiescence and suppress the development of hepatocellular carcinoma through inactivation of the Yap1 oncogene. *Cancer Cell*, *16*(5), 425–438. https://doi.org/10.1371/journal.pone.0178059

Zou, J.-J., Luo, H.-S., Huang, Z.-Y., Zeng, Q., & Wu, D.-H. (2011). Correlation of casein kinase

2β overexpression to the metastatic ability of colorectal cancer cells in vitro. *Journal of Southern Medical University*, *31*(4), 628–632.